HYDROGEOCHEMICAL, GEOPHYSICAL AND GEOLOGICAL ASSESSMENT OF THE RECHARGE ZONE OF GUARANI AQUIFER SYSTEM IN ALEGRETE, SOUTHERN BRAZIL

Wilmer Emilio García Moreno ⓘ * and Cássio Stein Moura ⓘ

Pontifícia Universidade Católica do Rio Grande do Sul – PUC-RS, Porto Alegre, RS, Brazil

*Corresponding author email: wilgm93@gmail.com

ABSTRACT. The state of Rio Grande do Sul has a huge part of the Guarani Aquifer, having a recharge area in its central and western region and, therefore, this investigation was focused on the city of Alegrete. There is no annual plan for water resources in the state and, hence, it is required to evaluate the hydrogeochemical, geophysical and geological characteristics where the aquifer has its recharge regions. Thus, some data were acquired, having chemical analysis of the water in different wells (mostly in rural areas) and refraction seismic and geoelectrical surveys. In addition, the geological information was obtained from the public database SIAGAS (Sistema de Informações de Águas Subterrâneas – ground water information system). Then, different maps of chemical parameters and a Piper diagram were made. Moreover, the refraction seismic and geoelectrical data were processed and interpreted, concatenating these results with the geological data obtained from the SIAGAS wells, mapping the different formations and static levels of the aquifer. A high concentration of lead, chromium and cadmium along with phosphate was found. Additionally, by means of geophysical surveys, a line was pointed out as a possible aquifer, which could be used for human, agropastoral or industrial activities after treatments of altered value.

Keywords: geophysical inversion; Piper diagram; dipole–dipole array; geoelectric method; refraction seismic

INTRODUCTION

Life comes from water that is more than a chemical formula (H_2O) and so its importance is indisputable, indispensable in daily life, and has a direct repercussion on the economy, energy industry (hydroelectric plants), manufacturing industry, agriculture and ecological and environmental activities (Gleick et al., 2004). For these reasons, water is the core of any sustainable development.

When we think about the future, it can be noticed that there are few positive panoramas about water availability in relation to its demand, which is strongly linked to the increase of the world population. Moreover, the industrial market and domestic consumption will need more water than the agricultural area, especially in developing countries (or regions) or emerging economies and here is where Brazil takes place in the world (UNESCO, 2018).

According to the Secretary of Planning, Budget and Management in the Socioeconomic Atlas of Rio Grande do Sul State (SPGG, 2019), the agriculture in Rio Grande do Sul (RS) contributed 12.1% to the Brazilian agricultural gross value, placing it in the first place among all the states in the country. In addition, in 2015, Rio Grande do Sul presented the largest irrigation area (ANA, 2017) while the groundwater was exclusively used for urban supply in more than 50% of the Brazilian towns (ANA, 2010). Analyzing the municipality of Alegrete, among the municipalities in Rio Grande do Sul and even in Brazil, Alegrete occupies the fourth place of the 1792 cities that produce rice (IBGE, 2020a). Also, it is the main municipality in Rio Grande do Sul that produces cow, ox and buffalo goods, besides being the third in the equine production in the state and the fifth in Brazil among 5518 municipalities (IBGE, 2020b), having water as the main resource to maintain these economical areas.

The Guarani Aquifer System (SAG) is the biggest transboundary aquifer in the world (CETESB, 2022). It is present in Brazil, Argentina, Paraguay and also in Uruguay covering an area of 840000 km² approximately, of which around 70% is located in Brazil, occurring in the states of Goiás, Mato Grosso, Mato Grosso do Sul, Minas Gerais, Paraná, Rio Grande do Sul, Santa Catarina and São Paulo. In total, more than 500 cities being supplied by the Guarani Aquifer and, due to its water quality, it has been used for the domestic, agricultural and industrial consumption (CPRM, 2008).

Due to the agricultural production and the relevance to RS and Brazil, as well as the hydrological potential in Rio Grande do Sul, the main objective of this work is to show the first investigations in the municipality of Alegrete by means of hydrogeochemical tests, geophysical surveys and mapping of geological formations, considering that Alegrete is one of the innumerous recharge zones and outcrop regions of the Guarani Aquifer System in the state of Rio Grande do Sul. Therefore, it was studied a part of the city of Alegrete seeking to carry out a hydrographic inventory as a first step for the water resource plan in the state.

Geological Settings

Alegrete is a borough located in the west of Rio Grande do Sul state, approximately 506 km from the capital, Porto Alegre (Figure 1). Most of the municipality is based on a basaltic province, and most of the rocks are formed by fissure volcanic spillovers, which occurred in the Paraná Basin in the Mesozoic Era, forming the Serra Geral Formation (Alves, 2008).

The fissural magmatism which caused the uplift of these rocks is related to the rupture of Gondwana, that is the opening of the Atlantic Ocean in the Lower Cretaceous (Zalán et al., 1987). Additionally, Martins et al. (2011) found six volcanic spillovers, forming the Serra Geral Formation (Figure 2). In addition to volcanism, it can be identified aeolian sandstones belonging to the Botucatu Formation (de Paula and Robaina, 2003), as well as the fine and conglomeratic sandstones of the Guará Formation and the sandstones/siltstones of the Sanga do Cabral Formation (de Paula, 2006). Also, in Botucatu Botucatu formation, it can be observed the Guarani Aquifer.

METHODOLOGY
Hydrogeochemical analysis

The samples were obtained in concordance to ABNT NBR 15847 (ABNT, 2010) from 21 different sites, which most of them were wells. When the acquisitions were not directly from wells, it was used a faucet near them. Also, to get the water samples from wells it was used a purging time of 10 minutes and the samples were acquired subsequently. After the acquisition, the water samples were stored at 4°C until the posterior analysis. The samples were acquired in southern winter, specifically between July 18 – 19 in 2018; 17 of the 21 wells were located in rural areas, where agricultural activities were carried out. In addition, the information of these wells is in Table 1.

Water Analysis

To obtain physicochemical parameters such as dissolved oxygen, electrical conductivity, and pH, the samples were measured in situ by means of a multiparameter equipment which had flow cells. In contrast, more two physicochemical parameters were calculated. However, the methods were different; the first was water hardness and the second was alkalinity and, for both of them, they were performed according to the Standard Methods (Clesceri et al., 1998). In the case of water hardness, it was used ionic chromatography and after, equation (1), the calculation of water harness.

$$CaCO_3 = \left[2.497 Ca\left(\frac{mg}{l}\right)\right] + \left[4.118 Mg\left(\frac{mg}{l}\right)\right] \qquad (1)$$

where

Ca = calcium concentration

2.497 = conversion from Ca to $CaCO_3$

Mg = Magnesium concentration

4.118 = conversion from Mg to $CaCO_3$

In the case of anions and cations, the measurement was made by ionic chromatography; notwithstanding, the equipment for both was different. In the case of anions, it was used the ICS 5000 and for the cations, the Dionex DX 500. The other analyzed parameter was concentration of metals; therefore, the technique was spectrometry of optical emission with plasma by means of the Perkin Elmer Optima equipment.
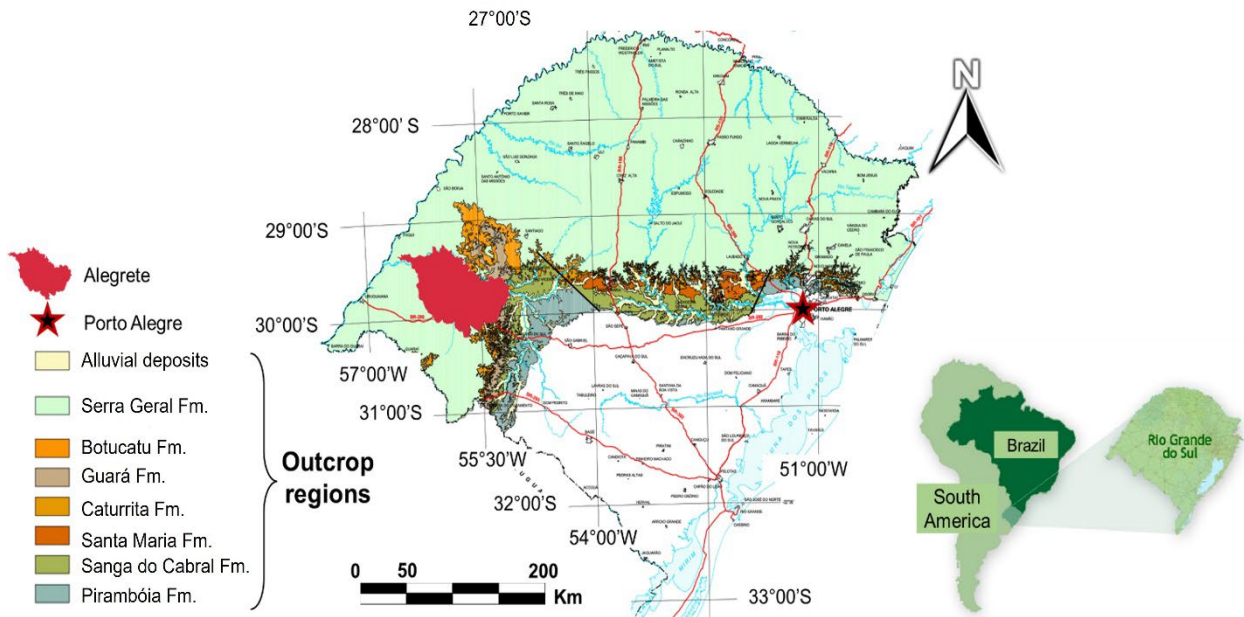
Figure 1: Rio Grande do Sul map showing the recharge zone of the Guarani Aquifer in the state and the location of Alegrete city. Modified from Flores Machado (2005).
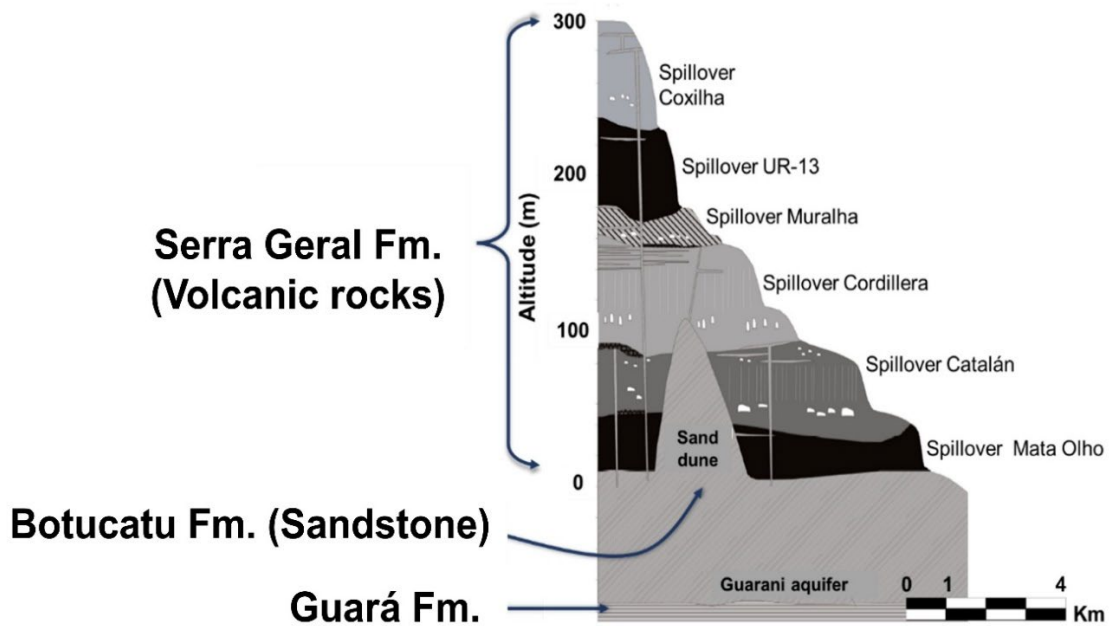
Figure 2: Formations (Fm.) in Alegrete. Modified from Martins et al. (2011).

Mapping of parameters

The area to be mapped was delimited taking into account the wells where the samples were taken. After that, they were gridded using the kriging method setting the convex hull to 500 m to not have a huge extrapolation. In addition, the maximum allowed hydrogeochemical parameters can be found in annex 1. In the case of the Piper diagram, it was used the OriginLab 2019; here, only the result of the measured ions was needed.

Geoelectric survey

Taking into consideration some authors that have worked for this method (Orellana, 1982; Telford et al., 1990; García et al., 2011), it is needed four electrodes (Figure 3), two as current electrodes (A and B) and two more as potential (M and N) having a potential difference named ΔV, seen in equation (2) and equation (3) Potential on the electrodes M and N. Moreover, it is required to consider the distance between

Table 1: Information of samples wells.

Well name	UTM X (21J)	UTM Y (21J)	Depth (m)	Area
EN_01	626474	6700118	–	Rural
EN_02	627679	6701226	–	Rural
PAI	609590	6694282	90	Rural
ALE	615292	6703006	–	Urban
JAC_01	608163	6713694	60	Rural
SAN_01	622193	6701897	40	Rural
SAN_02	622176	6701430	30	Rural
ESP_01	609921	6698931	114	Rural
INHA	598470	6692969	96	Rural
CAV_01	641701	6679193	–	Rural
CAV_02	639674	6679009	11	Rural
CAV_03	640612	6680214	43	Rural
CAV_04	618870	6700372	–	Rural
ALG_15B	620059	6703137	195	Urban
ALG_29	614353	6700855	120	Urban
ALG_30	619447	6702484	214	Urban
MAR_01	607615	6700593	72	Rural
MAR_02	607461	6700502	32	Rural
CAP	601401	6696673	–	Rural
VAS_01	605519	6692495	72	Rural
VAS_02	605997	6693019	63	Rural
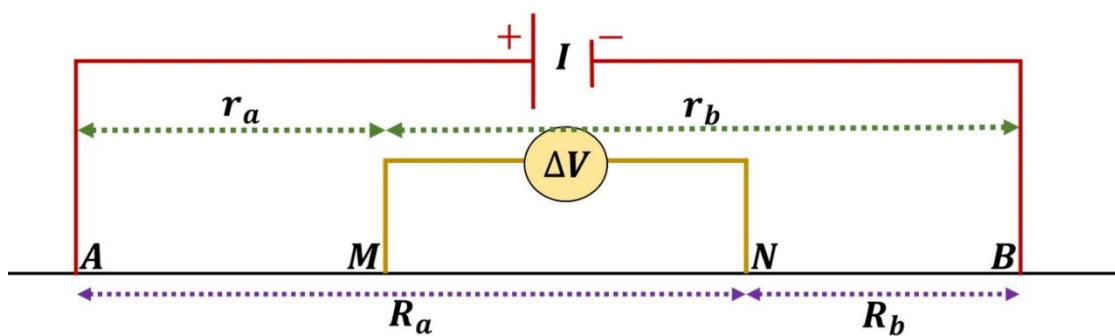
Figure 3: Generic array of the geoelectric method.

$\overline{AM} = r_A$; $\overline{MB} = r_B$; $\overline{AN} = R_A$ and $\overline{NB} = R_B$. Using all the distances between the electrodes inside the potential equations, it is obtained the geometric factor known as $k = \frac{2\pi}{\left(\frac{1}{r_A} - \frac{1}{r_B}\right)\left(\frac{1}{R_A} - \frac{1}{R_B}\right)}$. Having the geometrical factor and applying it to the potential difference, it is possible obtain Potential difference between M–N as equation (4) and deducing the equation (5) and equation (6), being them Resistivity on the array and Generic apparent resistivity.

$$\Delta V = V_C - V_D \tag{2}$$

$$\begin{cases} V_M = \dfrac{\rho I}{2\pi}\left(\dfrac{1}{r_A} - \dfrac{1}{r_B}\right) \\ V_N = \dfrac{\rho I}{2\pi}\left(\dfrac{1}{R_A} - \dfrac{1}{R_B}\right) \end{cases} \tag{3}$$

$$V_M - V_N = \dfrac{\rho I}{2\pi}\left[\left(\dfrac{1}{r_A} - \dfrac{1}{r_B}\right)\left(\dfrac{1}{R_A} - \dfrac{1}{R_B}\right)\right] \tag{4}$$

$$\rho = \dfrac{2\pi\Delta V}{I\left[\left(\dfrac{1}{r_A} - \dfrac{1}{r_B}\right)\left(\dfrac{1}{R_A} - \dfrac{1}{R_B}\right)\right]} \tag{5}$$

$$\rho_a = \dfrac{\Delta V}{I}k \tag{6}$$

For this survey, it was used a resistivity meter named X5xtal Control, using the dipole–dipole as acquisition matrix. Due to its acquisition and processing geometry and also because of its average horizontal and vertical resolution if compared to Wenner and Schlumberger methods (Cogon, 1973), it is necessary a 5 m space between the current electrodes (A–B), applying the same for the potential electrodes (M–N). Also, 100 m long arraying lines are needed, using the highest n=11. This acquisition is shown in Figure 4.

The software used to make the inversion of the data was the Res2Div 4.8.10. Here, the acquisition parameters were selected to make the inversion process, defining the stop criteria for 1% (error difference between two iterations less than 1%).

After obtaining the inversion file (.INV), it was used Surfer 13 to grid and generate the lines with better color degradation using a logarithmic scale and reducing the contour intervals. In this process the used method to grid was the inverse distance to a power, having zero convex hull, to not extrapolate the data out of the acquired points.

Refraction seismic survey

The seismic waves are propagated in the ground, interacting with different materials, making the waves being reflected, transmitted, and refracted (Telford et al., 1990) as they were surveyed. All these responses were registered by the geophones. By means of the first arrivals on radargrams, it is possible to obtain a model which can represent the layers below (Figures 5 and 6).

On the other hand, the first interpretation (in time domain) is given by the response of the direct waves, given by equation (7); after that, the travel time wave will be governed by equation (8) using a 1-layer model, equation (9) using a 2-layers model and for 3-layers model should be used the equation (10)

$$t_0 = \dfrac{x}{v_1} \tag{7}$$

$$t_1 = \dfrac{x}{v_2} + 2h_1\sqrt{\dfrac{1}{v_1^2} - \dfrac{1}{v_2^2}} \tag{8}$$

$$t_2 = \dfrac{x}{v_3} + 2h_1\sqrt{\dfrac{1}{v_1^2} - \dfrac{1}{v_3^2}} + 2h_2\sqrt{\dfrac{1}{v_2^2} - \dfrac{1}{v_3^2}} \tag{9}$$

$$t_3 = \dfrac{x}{v_4} + 2h_1\sqrt{\dfrac{1}{v_1^2} - \dfrac{1}{v_4^2}} + 2h_2\sqrt{\dfrac{1}{v_2^2} - \dfrac{1}{v_4^2}} + 2h_3\sqrt{\dfrac{1}{v_3^2} - \dfrac{1}{v_4^2}} \tag{10}$$

Six lines were surveyed in the same places where the geoelectrical surveys were made. The characteristics of these lines were 60 m long (the maximum extension of the cables), 12 geophones spaced every 5 m (due to the extension of the cable divided by the number of geophones) and 5 shotpoints spaced every 30 m. In each shotpoint it was made 3 measurements (3 gathers) to select the best, having a final arrangement as shown in Figure 7.

The acquisition consisted in five shotpoints, being the extreme points the shot offset. The software used to do the inversion was WinSeis 10. In here, firstly it is needed to pick the first arrivals; however, this step is done just in the shots two, three and four, and not in the shot offset. After this, it is analyzed the lines which represent the first picked arrivals, selecting the number of layers desired to model, being in this case, three layers. After this, it is selected the slopes which will give velocities and thickness to the layer. After the velocities being taken, the inversion is done, generating a .DAT, which will be gridded using the Surfer 13, as it was done in the geoelectrical inversion, with the same gridding method, notwithstanding the scale was linear and not logarithmic.

Geological mapping

Taking into account the hydrogeochemical study and the geophysical surveys, it was delimited the region to be mapped. Having already the coordinates, it was selected the wells which had information about the geological formations and it was defined the static level where the water was found. After this investigation, 91 wells were established. To model those wells and create the maps, it was used the software Surfer 13 and the gridding method to map was inverse distance to a power, selecting for every map *No Data convex hull of data* and *inflate convex hull at 500 m*, to not excessively extrapolate the maps, avoiding more uncertain results.
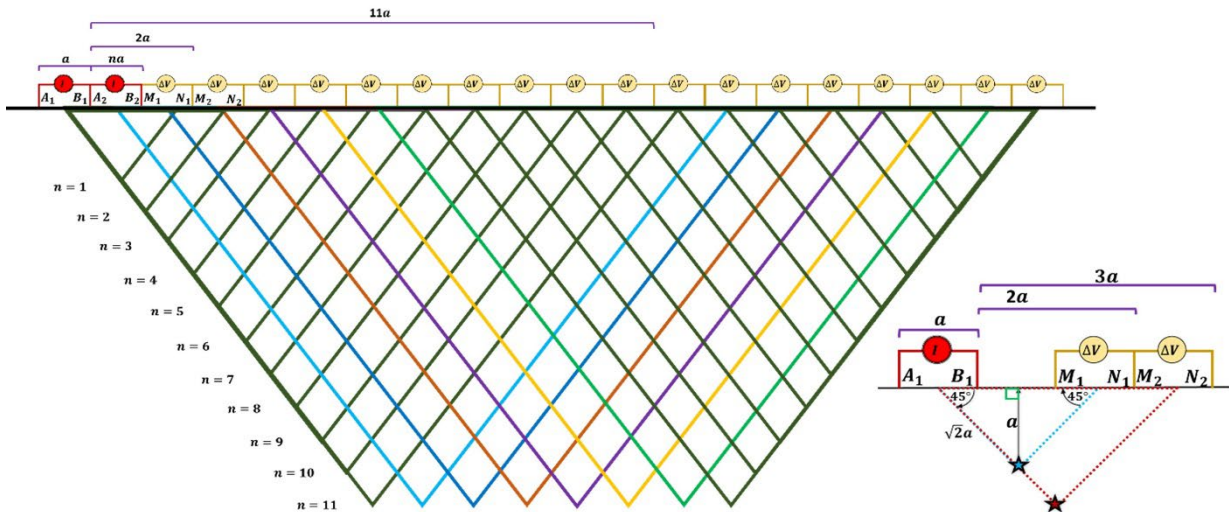
Figure 4: Illustration of the acquisition.
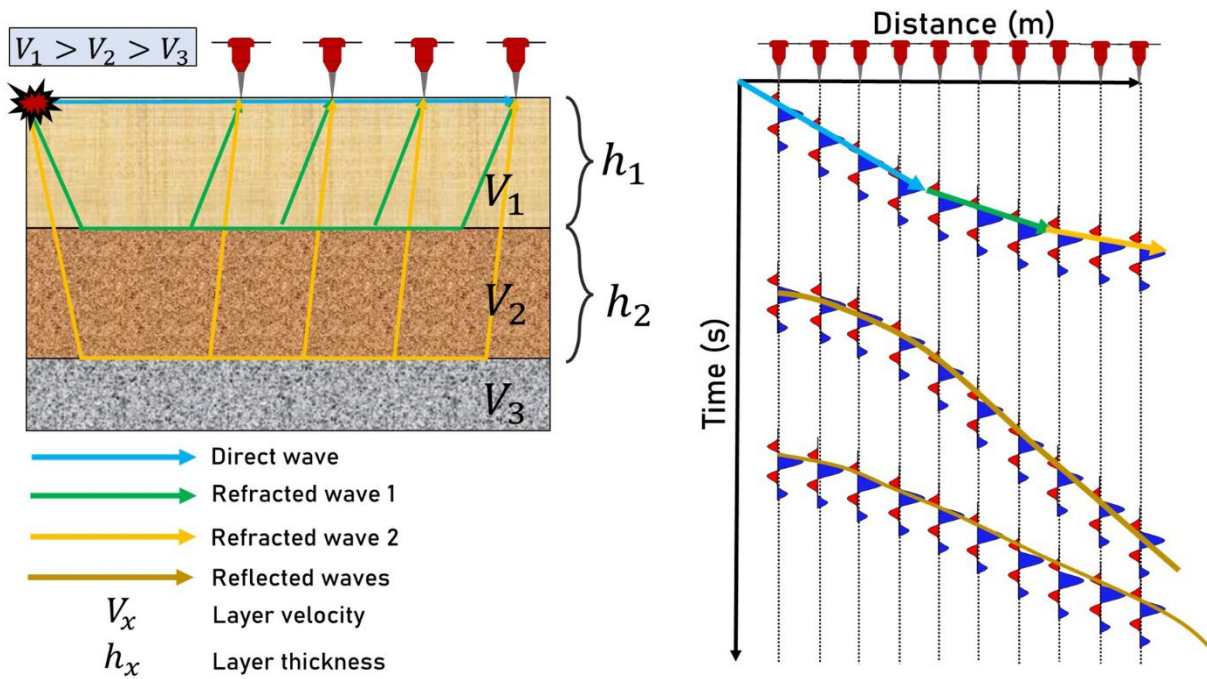
Figure 5: Acoustic waves in seismic acquisition.
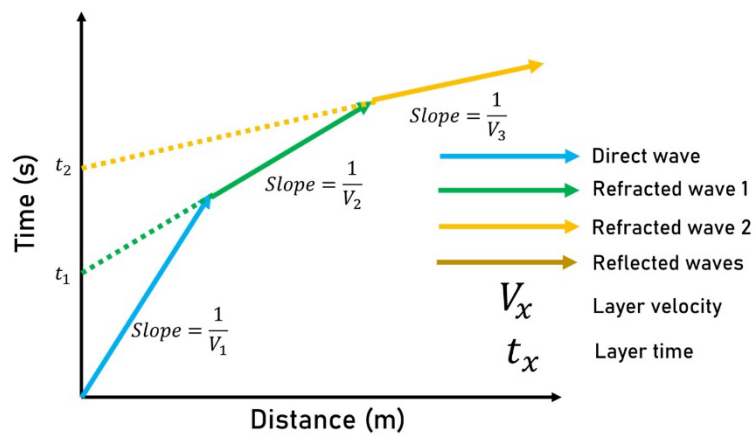
Figure 6: Refracted wave graph.
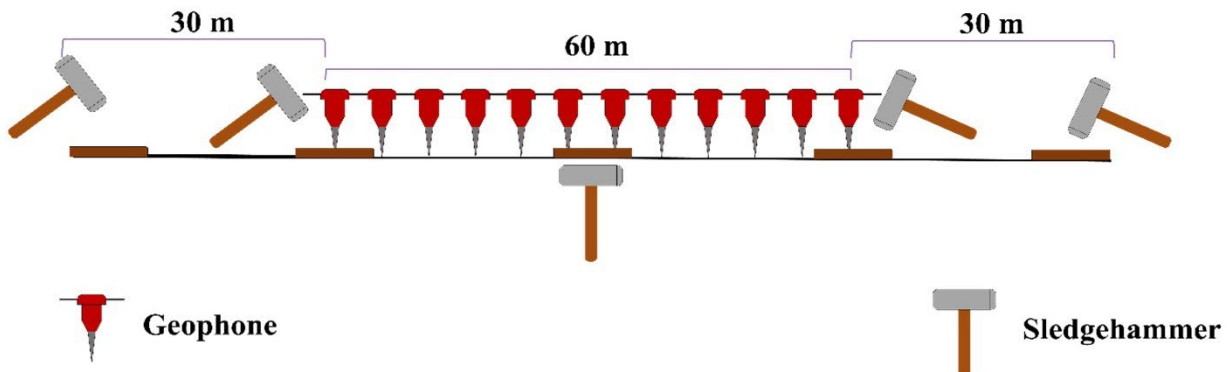
Figure 7: Acquisition of refraction seismic.

RESULTS AND DISCUSSION

This investigation was based on data about water geochemistry, geophysics and geology from the national well database SIAGAS maintained by CPRM, related to the study area presented in Figure 8. Firstly, the hydrogeochemical parameters were mapped to notice the concentration behaviours along the analysed town and to perceive how much polluted was the water if a possible reservoir were found. After, the geophysical data were processed and analysed having as primordial objective to obtain the first overviews in this area. Also, as a complement of all of this, the geological data were modelled by different contour maps, showing the regional behaviour of geological formations and the aquifer system. Yet, the geological faults were not contemplated.

Hydrogeochemistry

The hydrogeochemistry information came from the water analysis of 21 wells, making 25 contour maps to observe the spatial behavior of the different chemical parameters, which were divided in:

- **Physicochemical parameters:** water alkalinity, electrical conductivity, water hardness, dissolved oxygen concentration and pH.
- **Anions:** bromine, chloride, fluoride, phosphate, nitrate and sulfate concentrations.
- **Cations:** calcium, magnesium, potassium and sodium concentrations.
- **Metals:** aluminum, arsenic, barium, cadmium, lead, copper, chromium, iron, manganese, selenium and zinc concentrations.

Also, a Piper diagram was made to correlate the geology and the chemical parameters of the water.

Physicochemical parameters

Four physicochemical parameters were analyzed in Alegrete. The maps and their values are shown in Figures 9, 10, 11 and 12 (the pink dot areas are the geophysical survey locations and the black stars refer to the measured wells), showing that no excess was observed in the parameters and that the closest parameters to the limit was only alkalinity.

Raju et al. (2014) mention (in an investigation in Godavari, India) that water hardness and alkalinity could be affected due to the geology of the area and the percolation of water coming from rain because rain tends to dissolve some minerals more easily. Therefore, it is supposed that CO_3, HCO_3 and CO_2 were the main ions that elevated the water alkalinity, a fact reflected after in the Piper diagram.

Anions

The anion concentration maps are shown in Figures 13, 14, 15, 16, 17 and 18. It can be noticed that the phosphate concentration is above the limit in almost all studied wells, while high nitrate concentrations were found outside the limits in two wells. Soares (2019) mentions that the high concentration of fluorides and phosphates may be due to natural processes such as the dissolution of the rock and the nitrate concentration may be attributed to fertilizers, a fact pointed out by Wick et al. (2012). Also, the phosphate concentration in groundwater also might be attributed to overlying soils, agricultural fertilizer, animal waste, leaking septic systems and infiltration of wastewater according to Welch et al. (2010) and Rao and Prasad (1997).

Also, in a study carried out in RS by *Universidade Regional Integrada do Alto Uruguai e das Missões* (Tiecher, 2017), it is mentioned that a liquid manure from swine has been applied as fertilizer because it is a macronutrient for plants; however, when the concentration is high , it can become accumulated in the soil, polluting the groundwater. Therefore, due to the Alegrete having an enormous agricultural activity in its territory (IBGE, 2020a), fertilizers might be pointed out as a main factor in phosphate and nitrate high concentration.
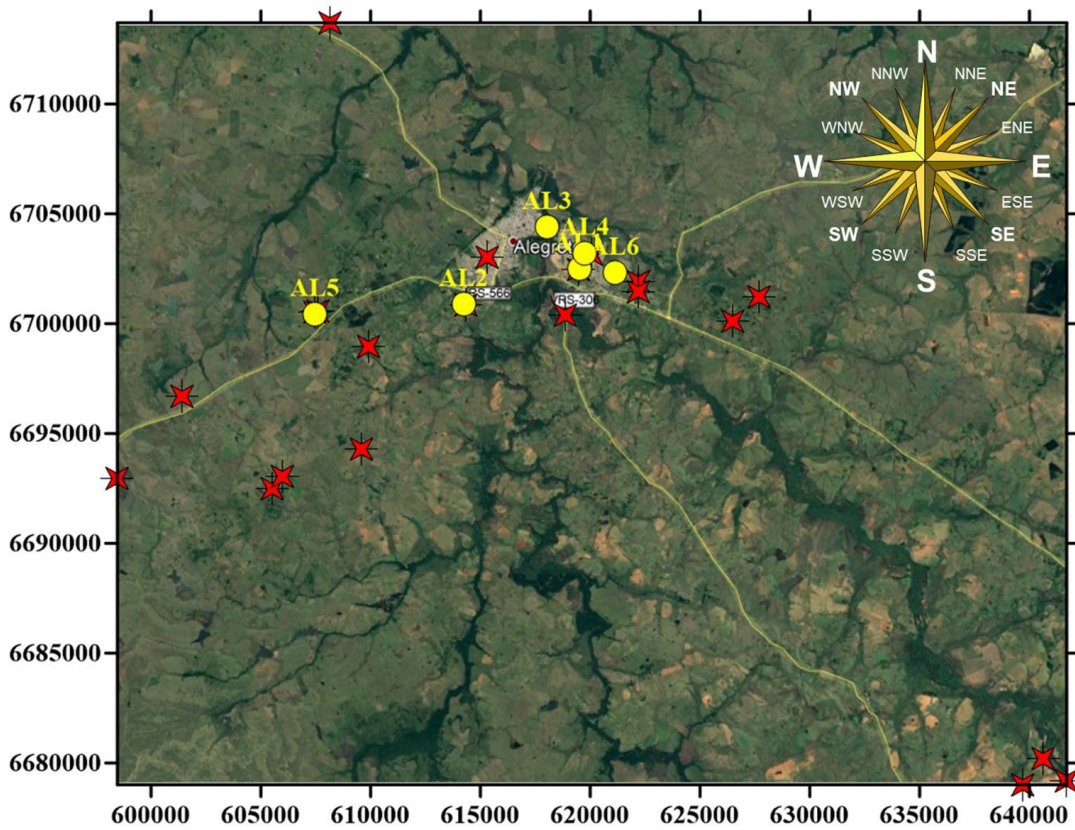
Figure 8: Location of the study area, where yellow dots indicate the geophysical surveys and red stars indicate where the chemical parameters were obtained.

Alkalinity (max = 200 mg/l)
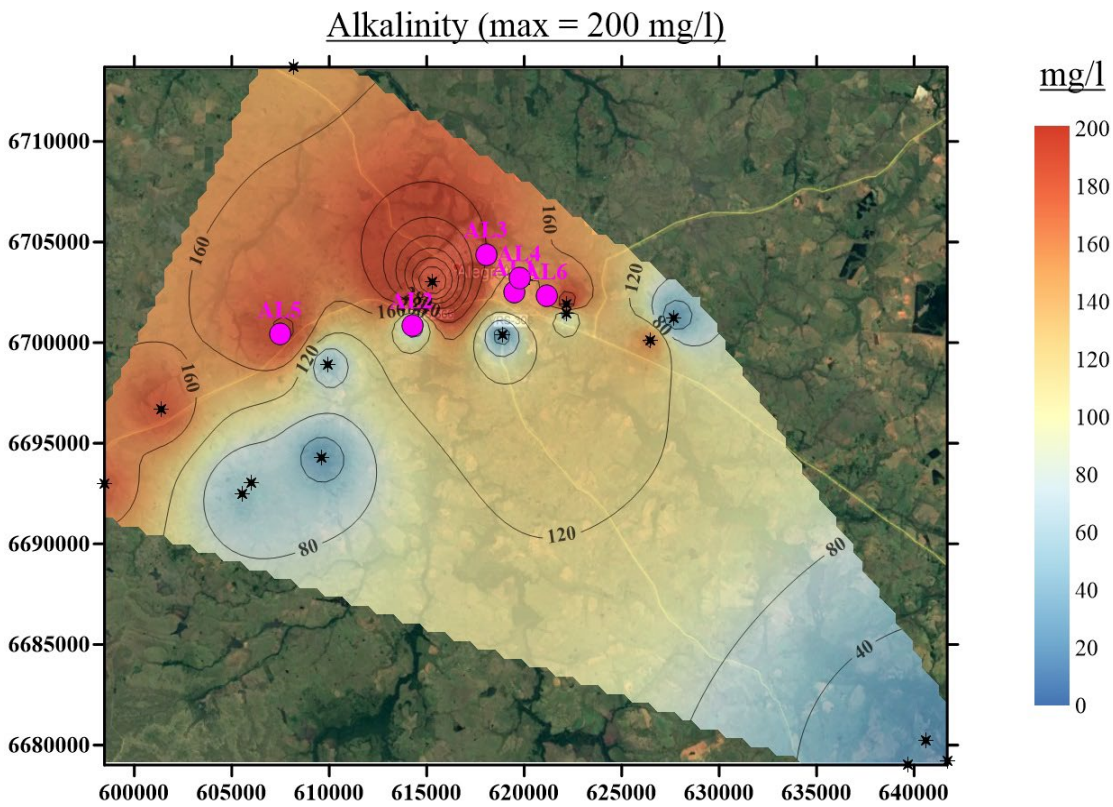
Figure 9: Water alkalinity.
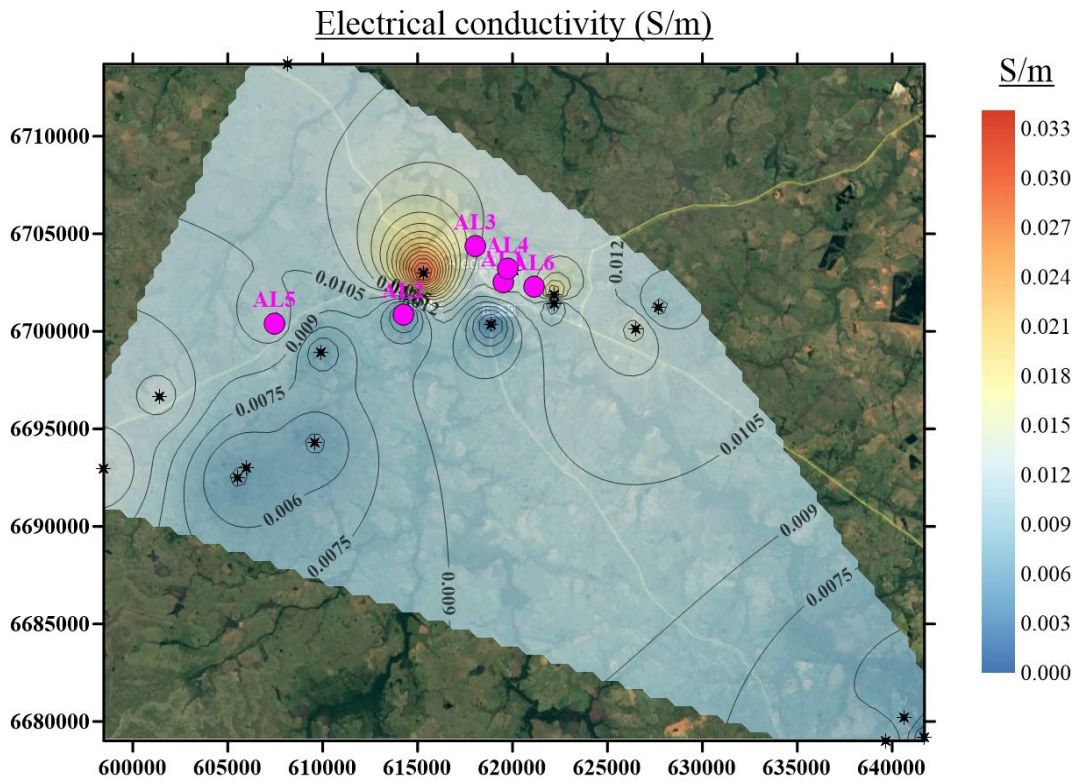
Figure 10: Water electrical conductivity.

Figure 11: Water pH.

Water hardness (max = 500 mg/l)

Figure 12: Water hardness.

Bromine concentration (max = 500 μg/l)

Figure 13: Bromine concentration.
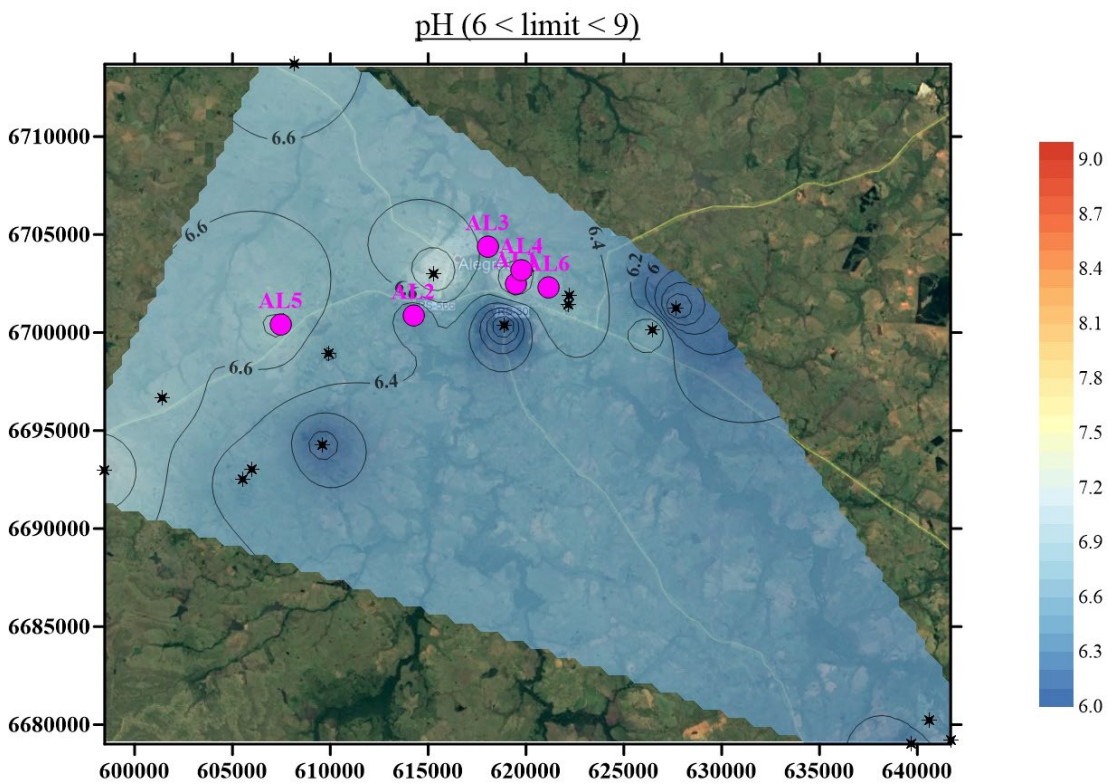
Chloride concentration (max = 250 mg/l)
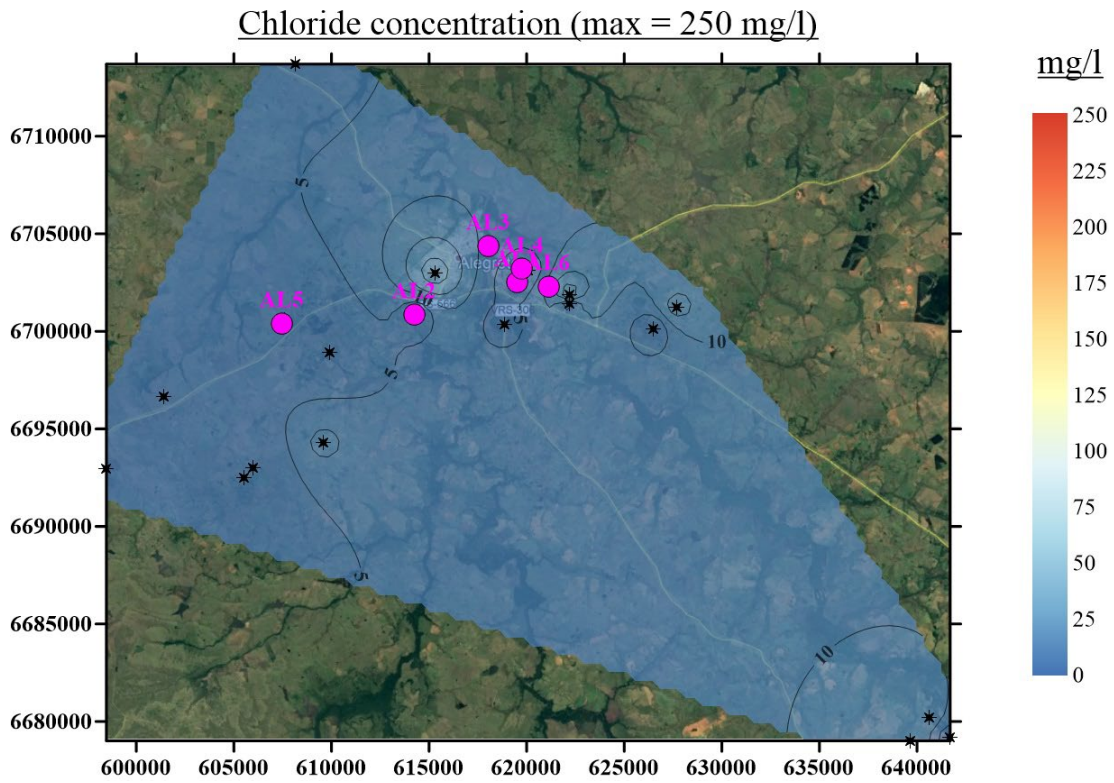
Figure 14: Chloride concentration.

Fluoride concentration (max = 1.5 mg/l)
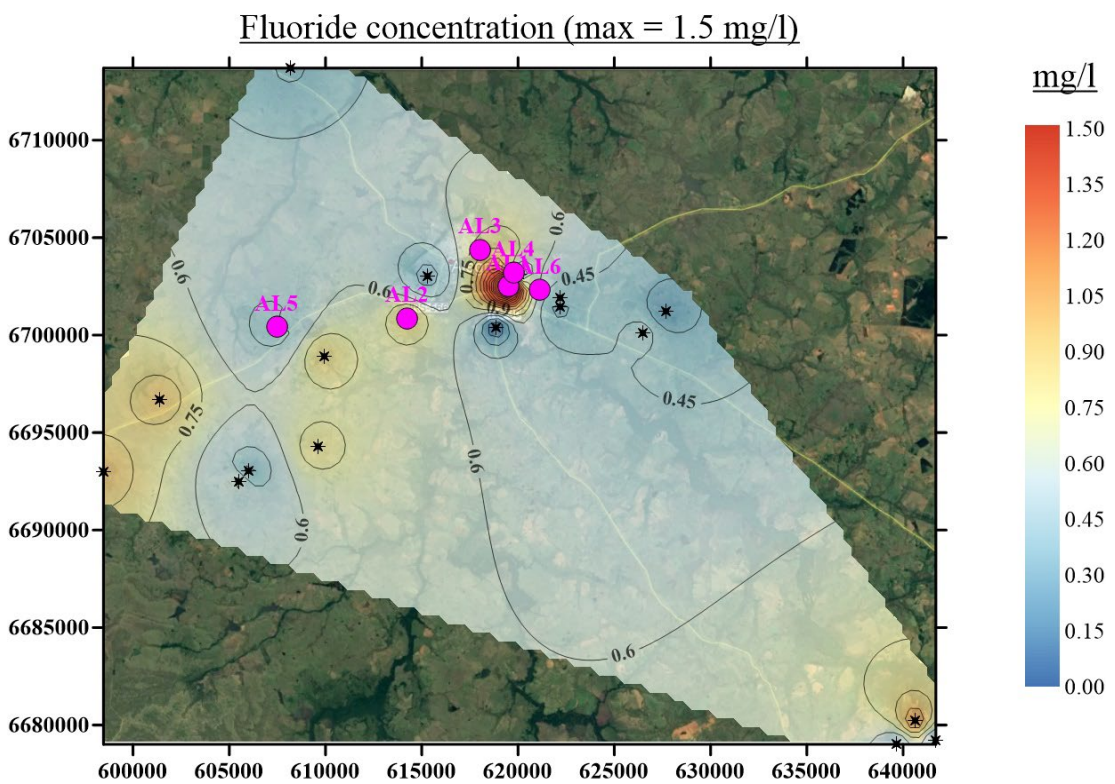
Figure 15: Fluoride concentration.

Nitrate concentration (max = 10 mg/l)
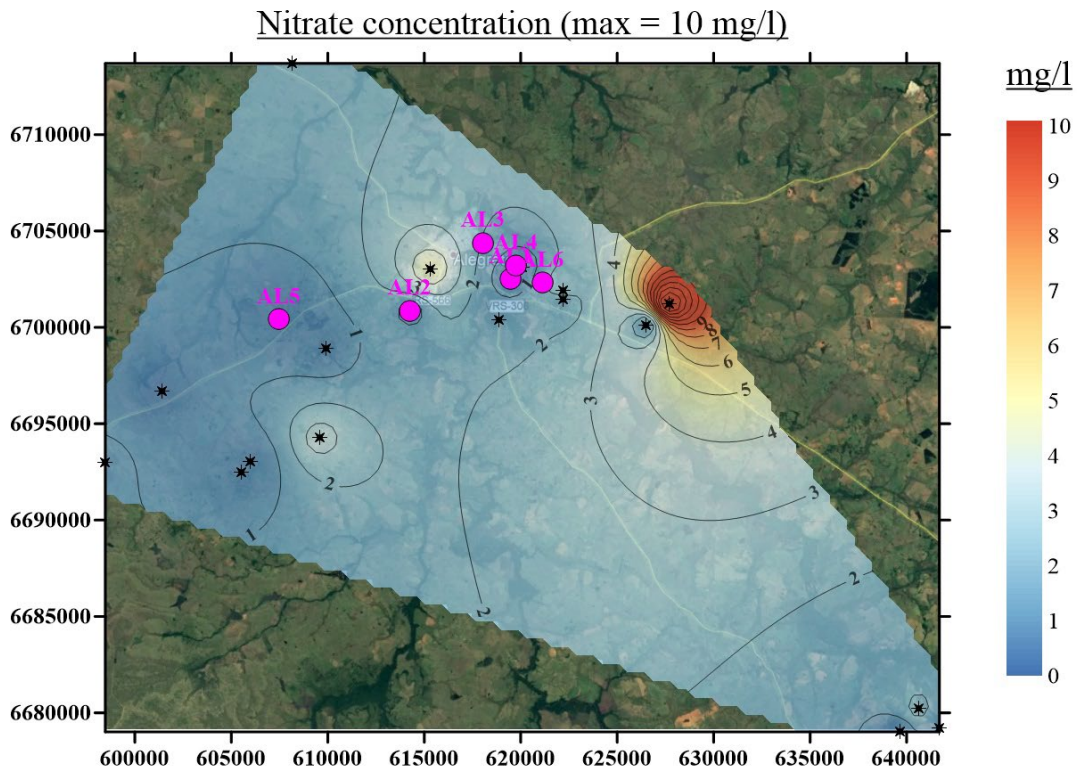
Figure 16: Nitrate concentration.

Phosphate concentration (max = 0.45 mg/l)
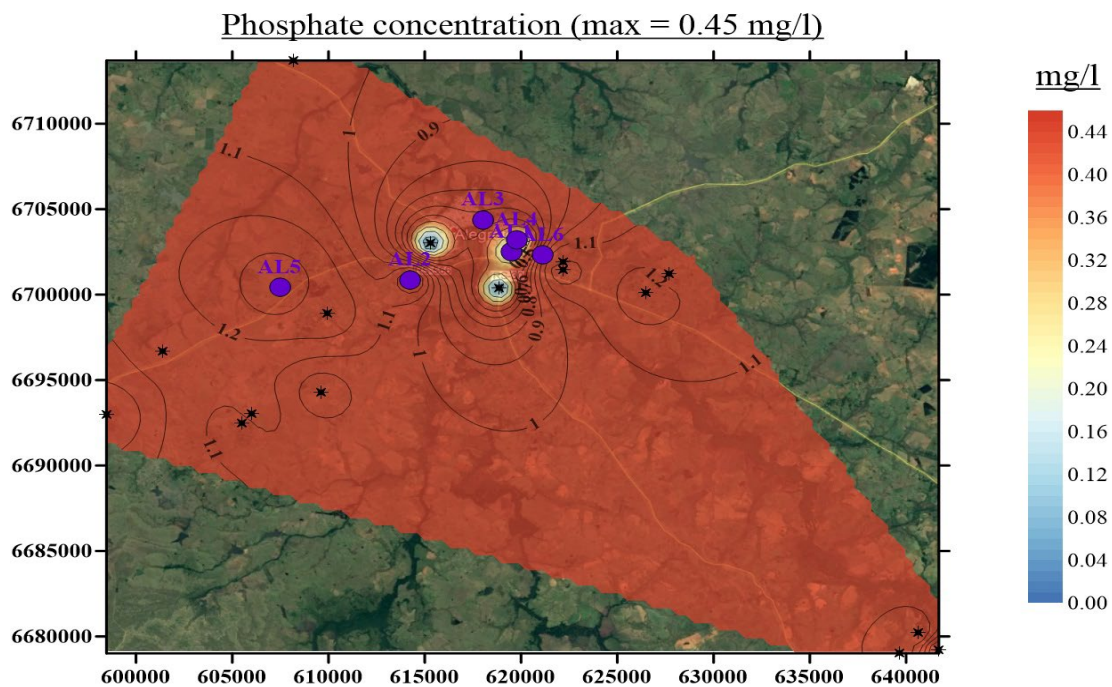
Figure 17: Phosphate concentration.

Sulfate concentration (max = 250 mg/l)
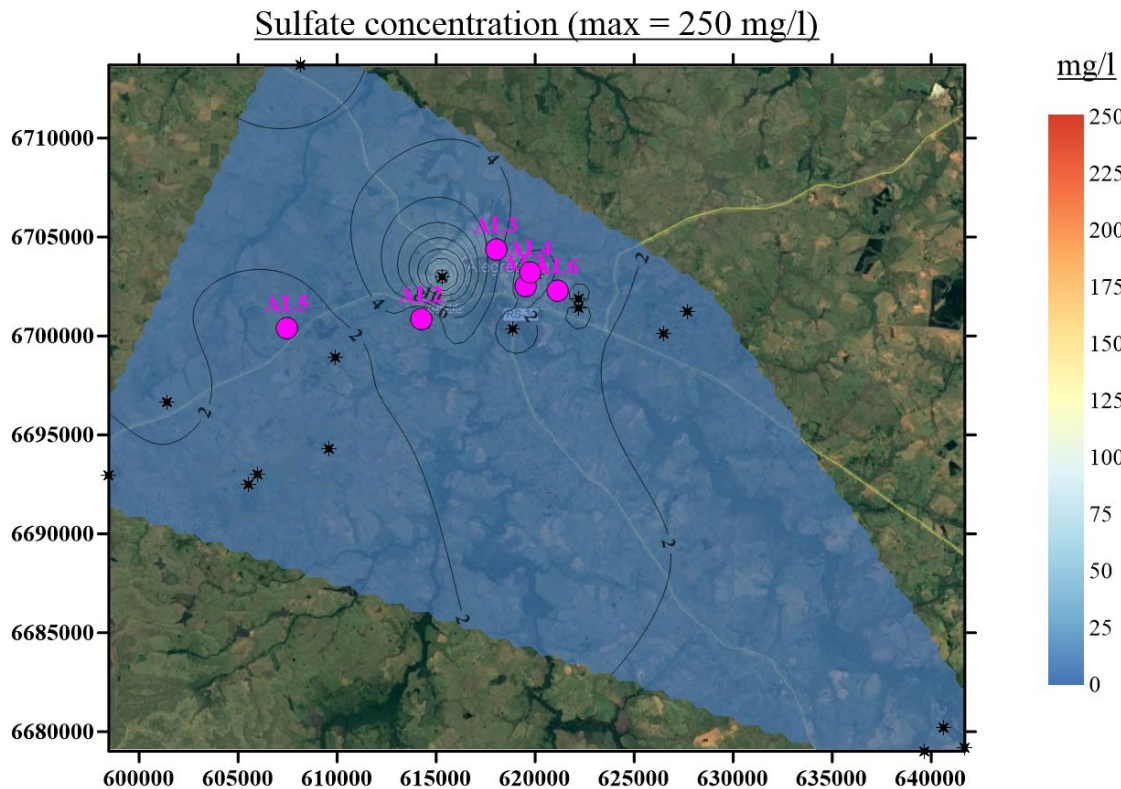
Figure 18: Sulfate concentration.

Cations

The cation concentration maps in the Alegrete region are shown in Figures 19, 20, 21 and 22. It was observed that all of them presented values within the limits. However, it was perceived that the well with the highest concentrations of calcium and magnesium was also the one which had the highest value in water hardness, then, as explained before, the swine could be the main cause, due to some nutrients provided to them in addition to the daily food, as nutritional complement. Among these nutrients it can be found Ca, Mg, P, Na, Fe, Cu, Zn, Mn, I and Se. Only around 50% of the nutrients is processed and the rest is eliminated as manure which could posteriorly be used as fertilizer (Tiecher, 2017).

Metals

In the region studied in Alegrete, a total of ten metals were quantified in the well water samples. Their concentrations are shown in Figs 23, 24, 25, 26, 27, 28, 29, 30, 31, 32 and 33. It was noted high cadmium, lead and chromium concentrations in all wells, which may have health repercussions if this water is ingested without previous treatment. In addition, one well had values above the copper concentration limit.

The cadmium high concentration in groundwaters could be caused by industries that work with fossil fuels, pigments, batteries, solders, electronic equipment or lubricants, as mentioned by Alves et al. (2004). In the case of lead and chromium, the same origin was pointed out by the Water Treatment Portal (Portal de Tratamento de Água, 2008) and the Minnesota Pollution Control Agency (MPCA, 1999).

Also, following the suggestion given by *Universidade Regional Integrada do Alto Uruguai e das Missões* (Tiecher, 2017), RS was the state which presented the highest percentage of contaminated groundwater in Brazil, around 50%, and one of the main reasons was the fecal slurry by swine used as fertilizer, increasing elements like As, CD, Cr, Hg and Pb. Additionally, analyzing the reference, another reason could be the fluids from the equipments used to do agricultural activities.

Piper diagram

With the hydrogeochemical data of the wells in the Alegrete municipality, a Piper diagram was built (Figure 34) to discriminate their waters. Observing it, in general, the waters are carbonated divided into magnesian and sodic. Due to the fact that they are

Calcium concentration (max = 100 mg/l)
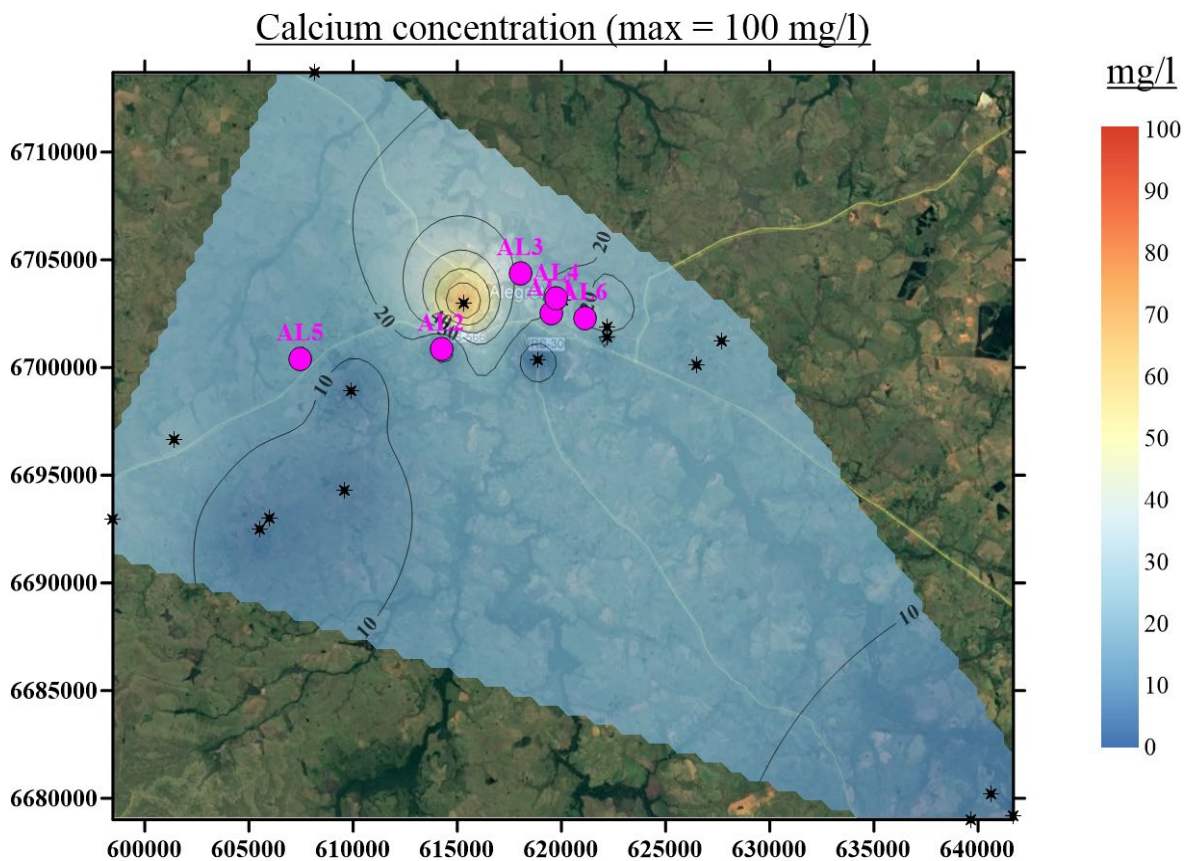
Figure 19: Calcium concentration.

Magnesium concentration (max = 30 mg/l)
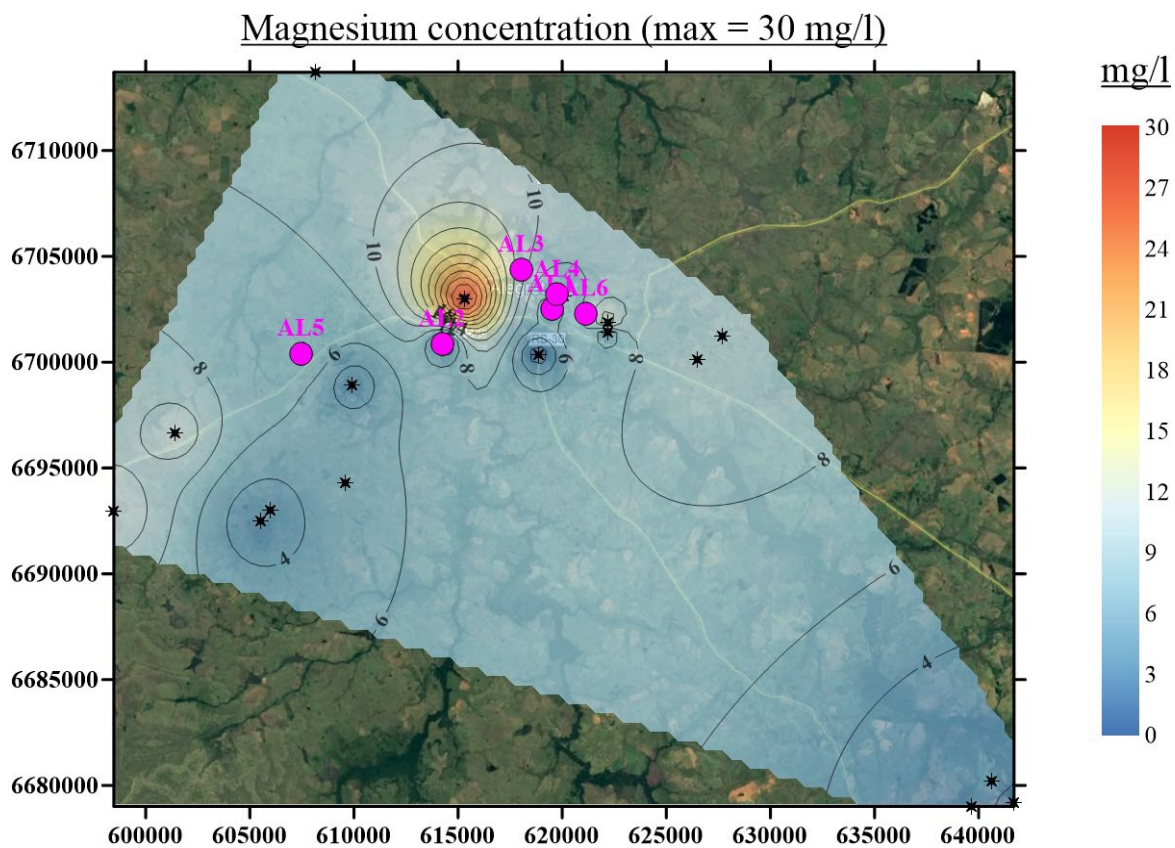
Figure 20: Magnesium concentration.

Potassium concentration (max = 10 mg/l)
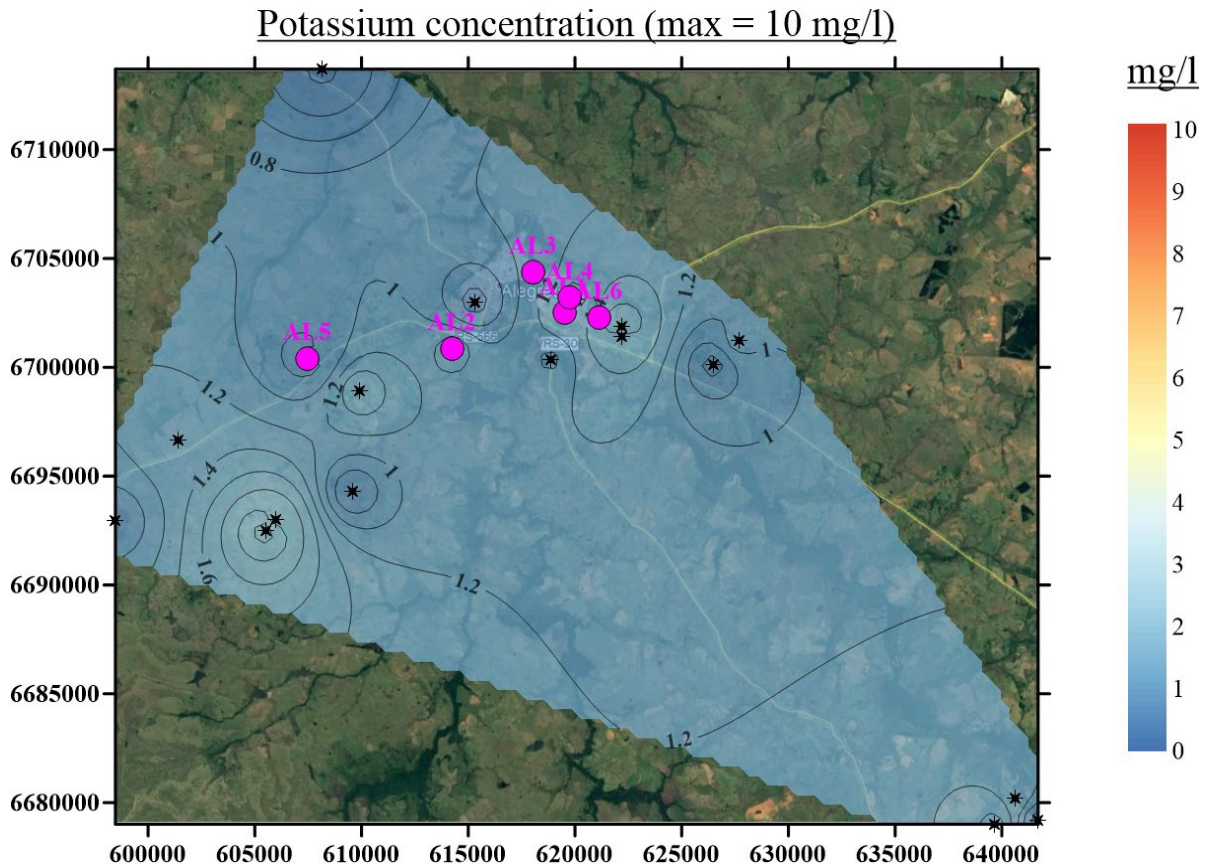
Figure 21: Potassium concentration.

Sodium concentration (max = 200 mg/l)
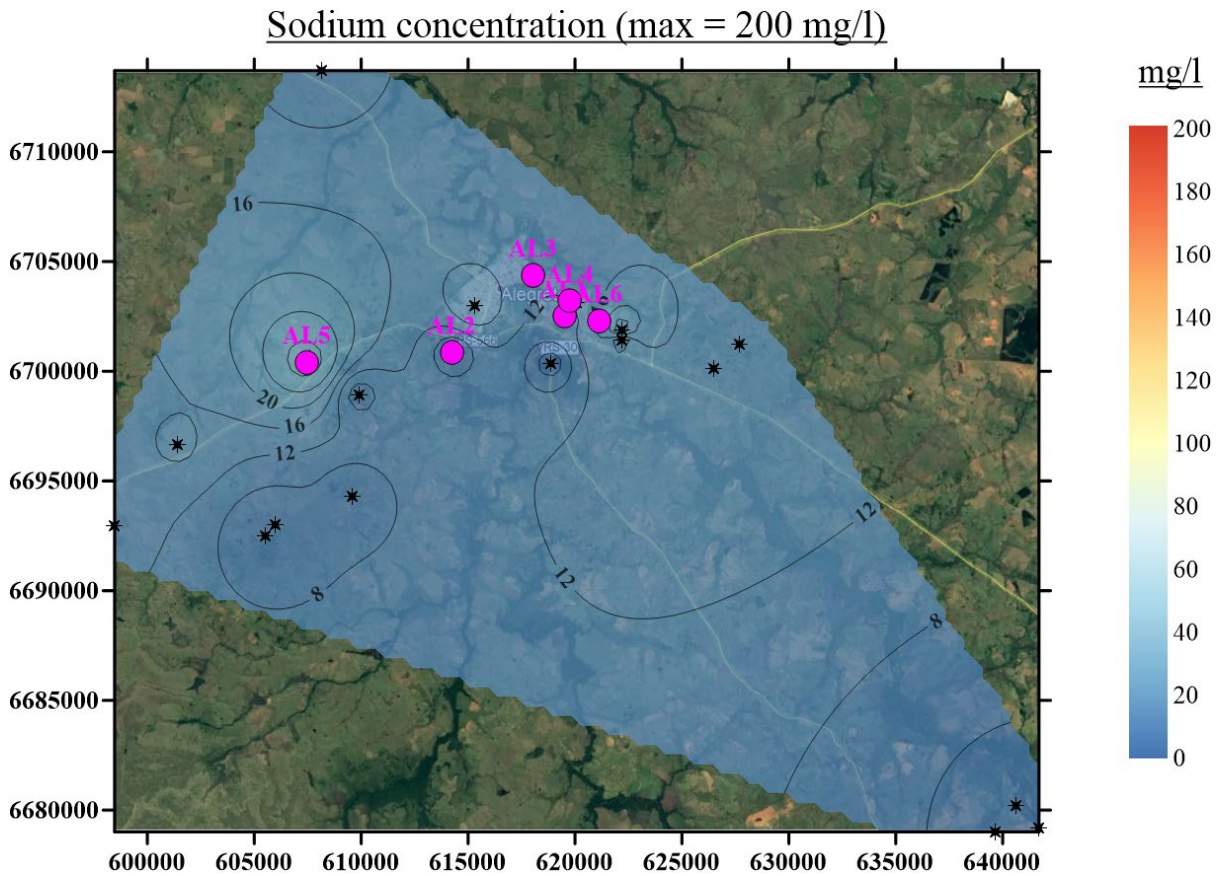
Figure 22: Sodium concentration.

Aluminium concentration (max = 200 µg/l)
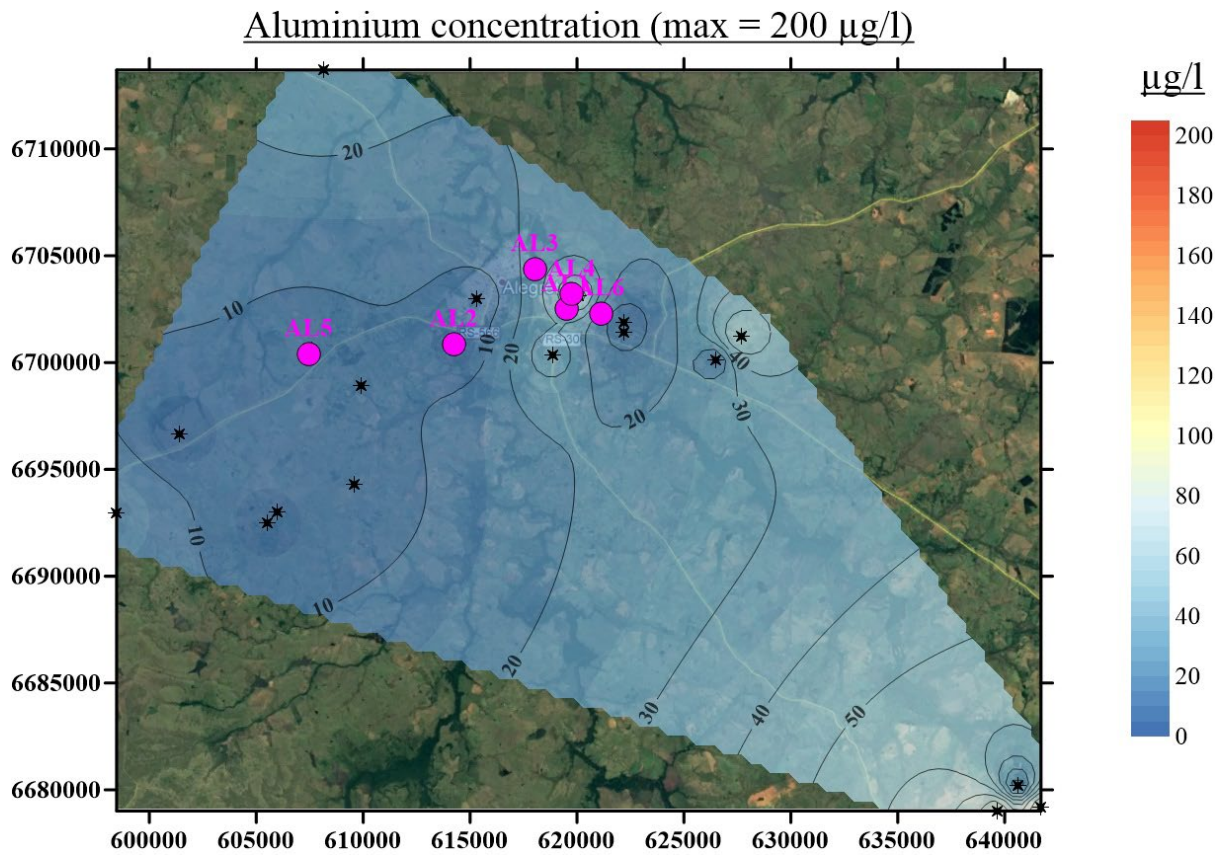
Figure 23: Aluminum concentration.

Arsenic concentration (max = 10 µg/l)
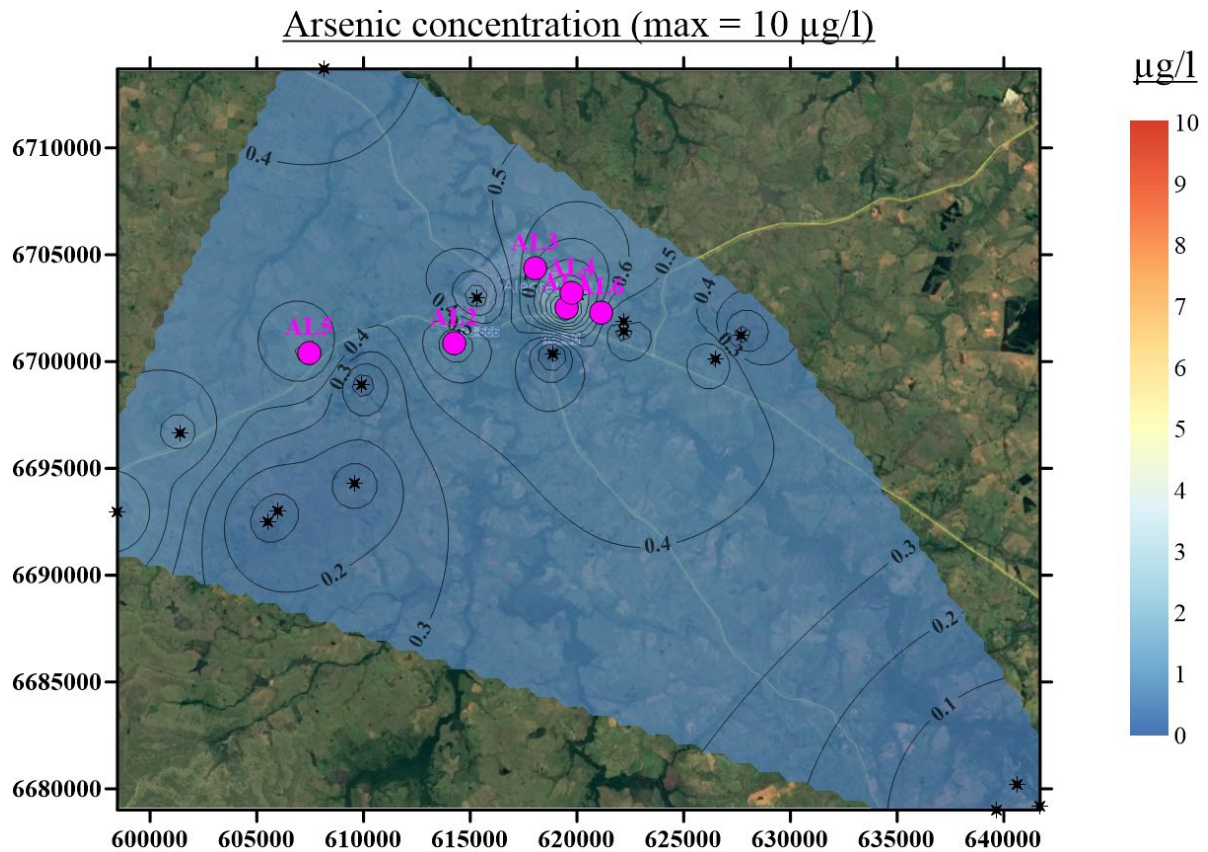
Figure 24: Arsenic concentration.

Barium concentration (max = 700 µg/l)
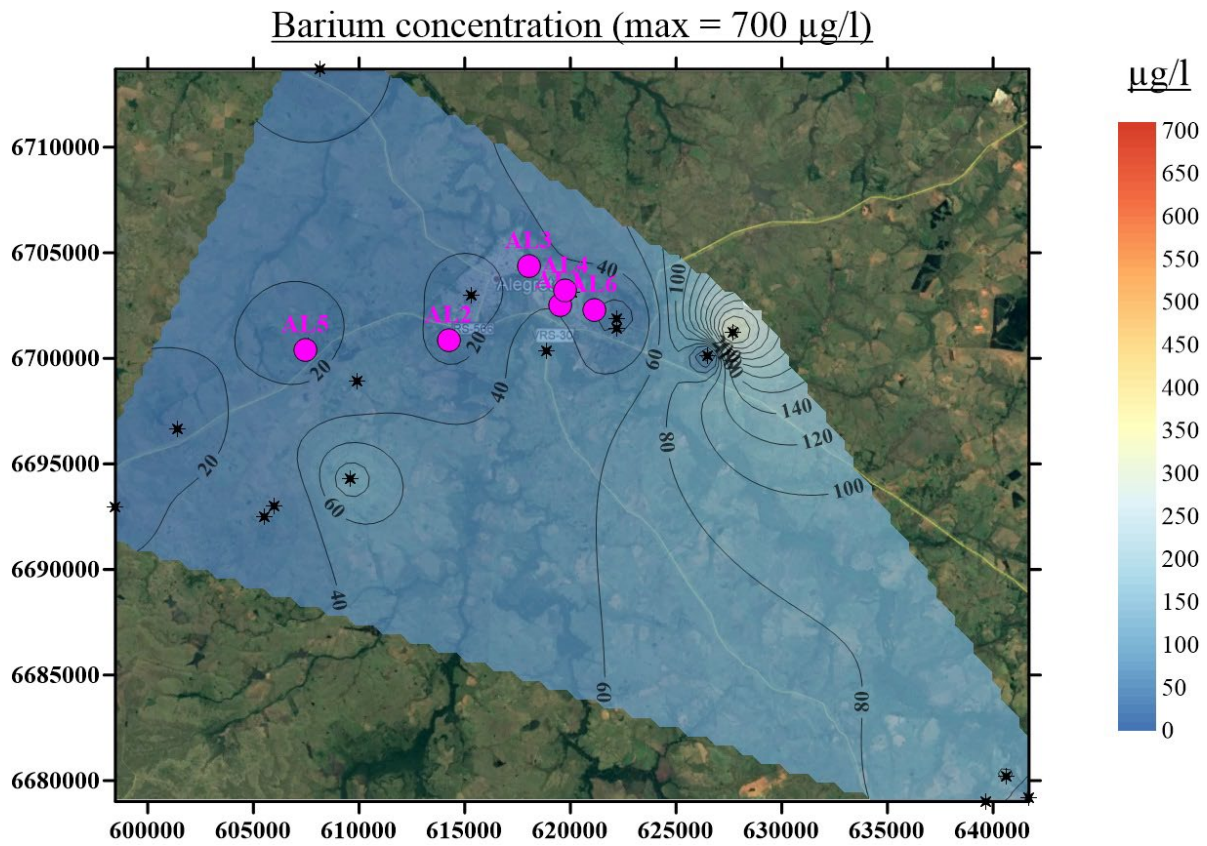
Figure 25: Barium concentration.

Cadmium concentration (max = 5 µg/l)
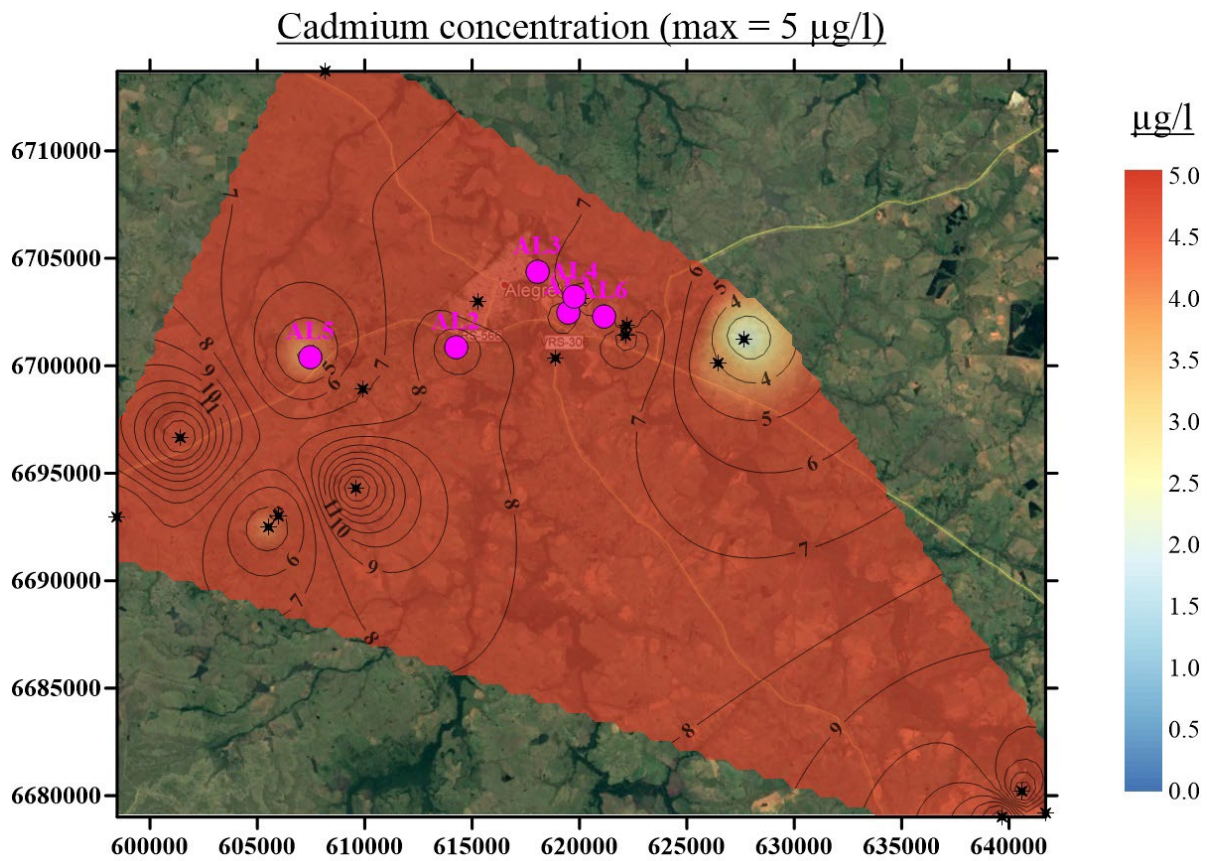
Figure 26: Cadmium concentration.

Chromium concentration (max = 50 µg/l)
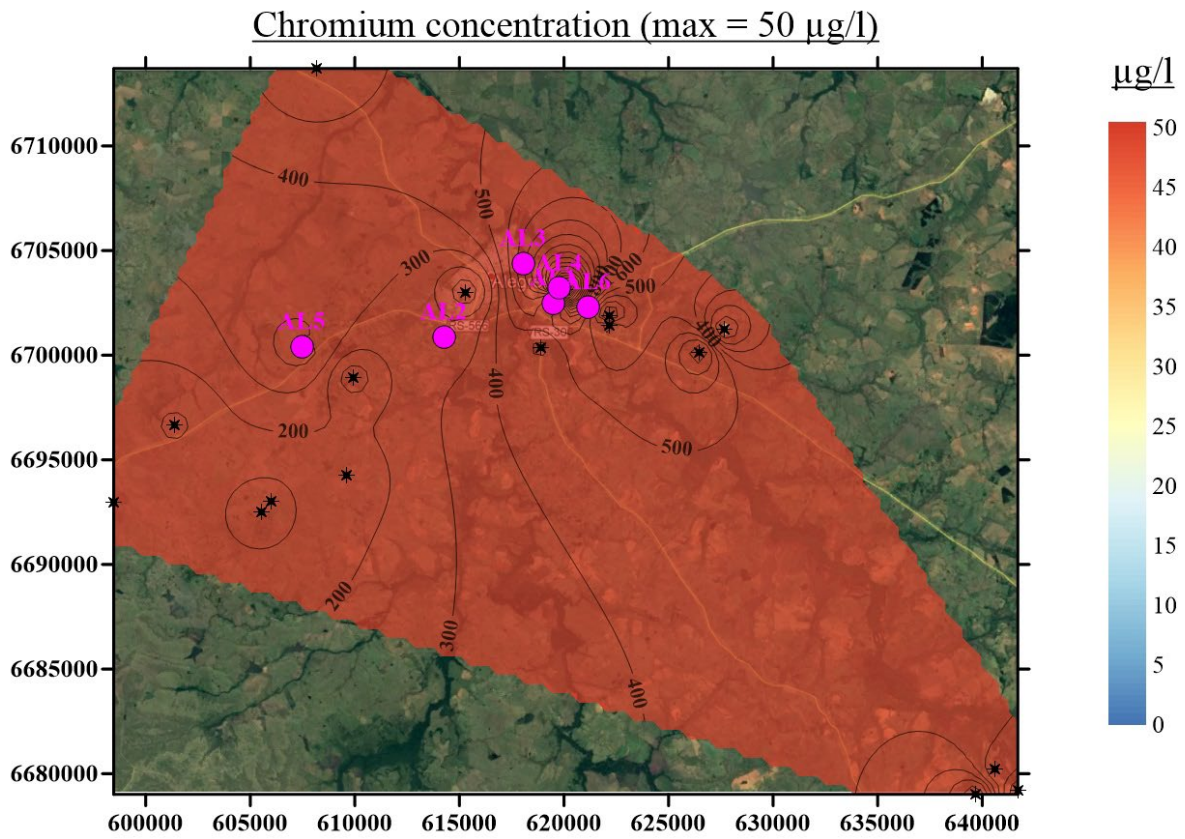
Figure 27: Chromium concentration.

Copper concentration (max = 2000 µg/l)
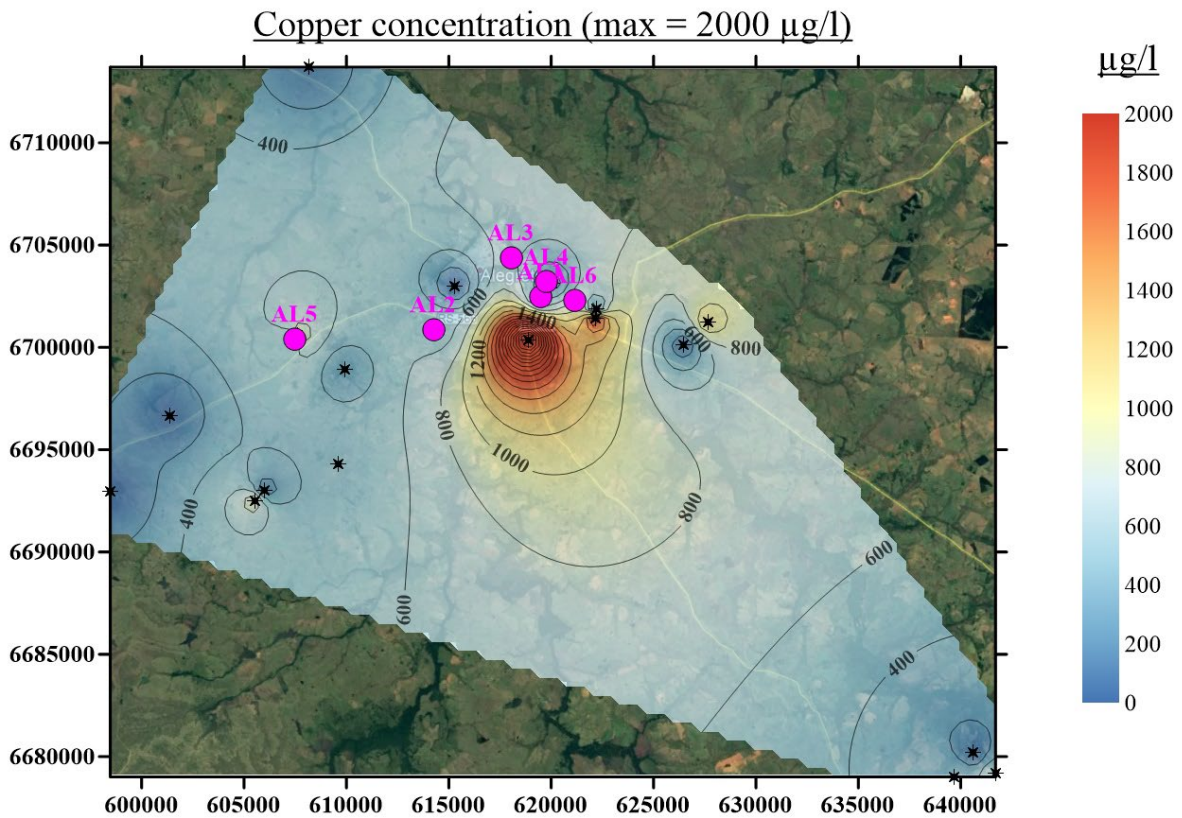
Figure 28: Copper concentration.

Iron concentration (max = 300 µg/l)
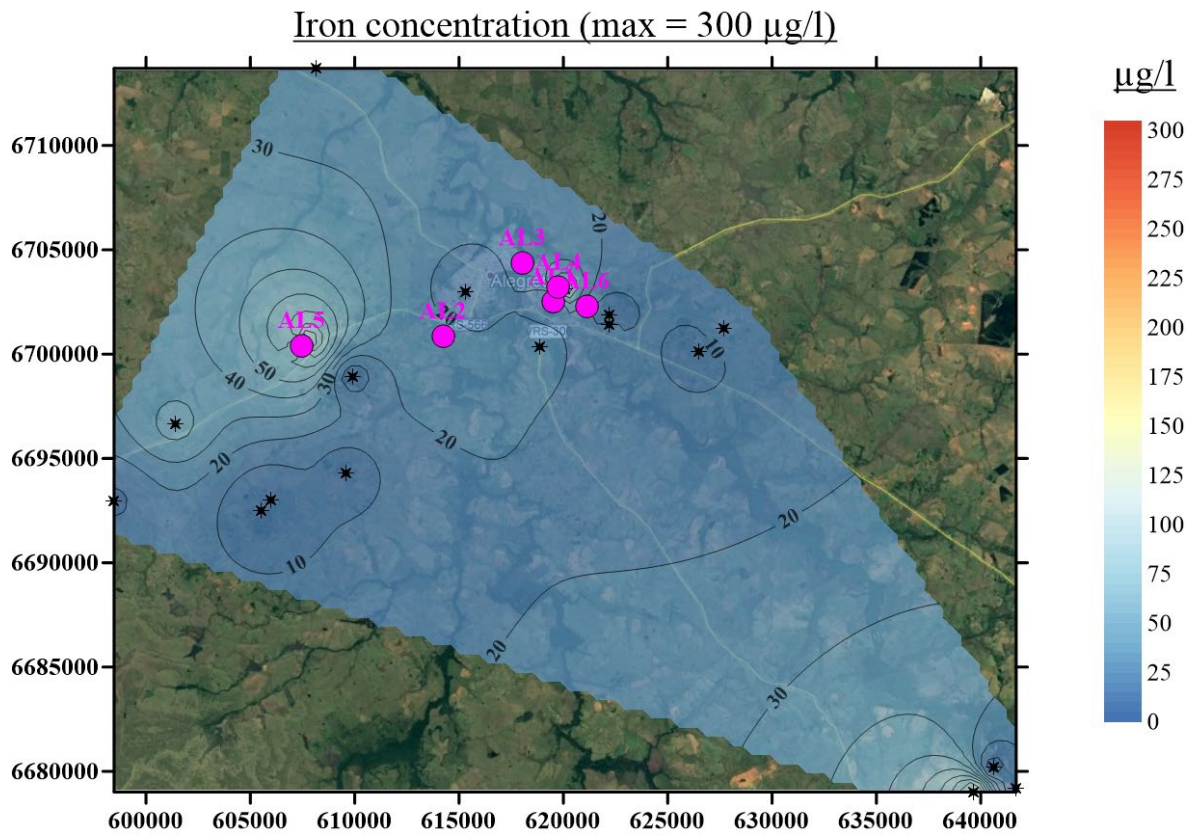
Figure 29: Iron concentration.

Manganese concentration (max = 100 µg/l)
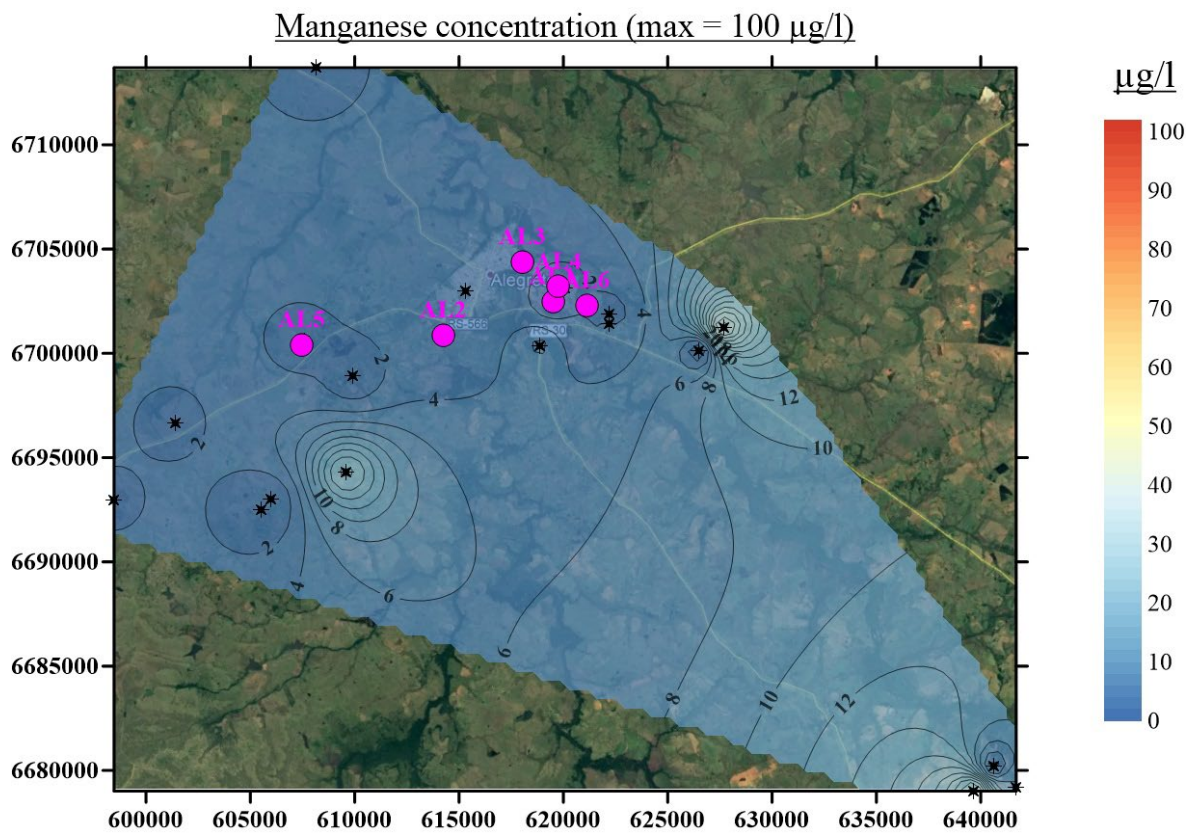
Figure 30: Manganese concentration.

Lead concentration (max = 10 µg/l)
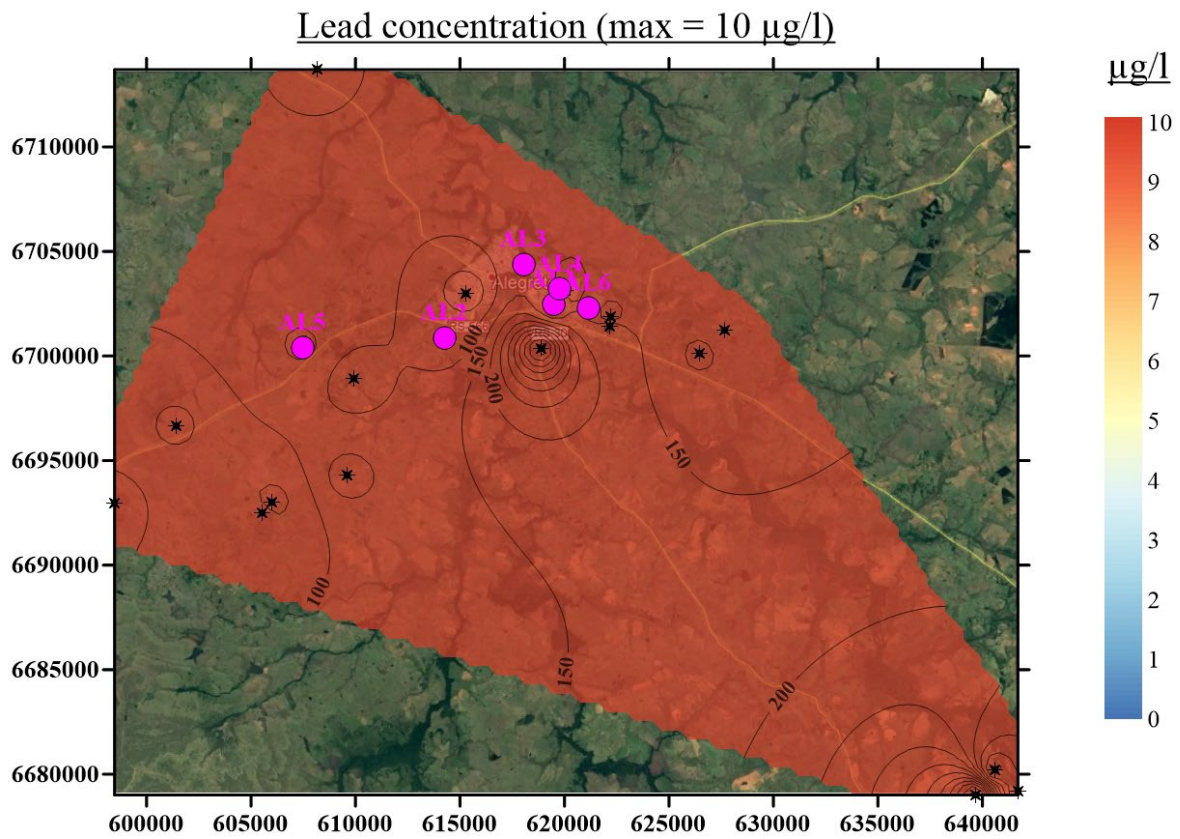
Figure 31: Lead concentration.

Selenium concentration (max = 10 µg/l)
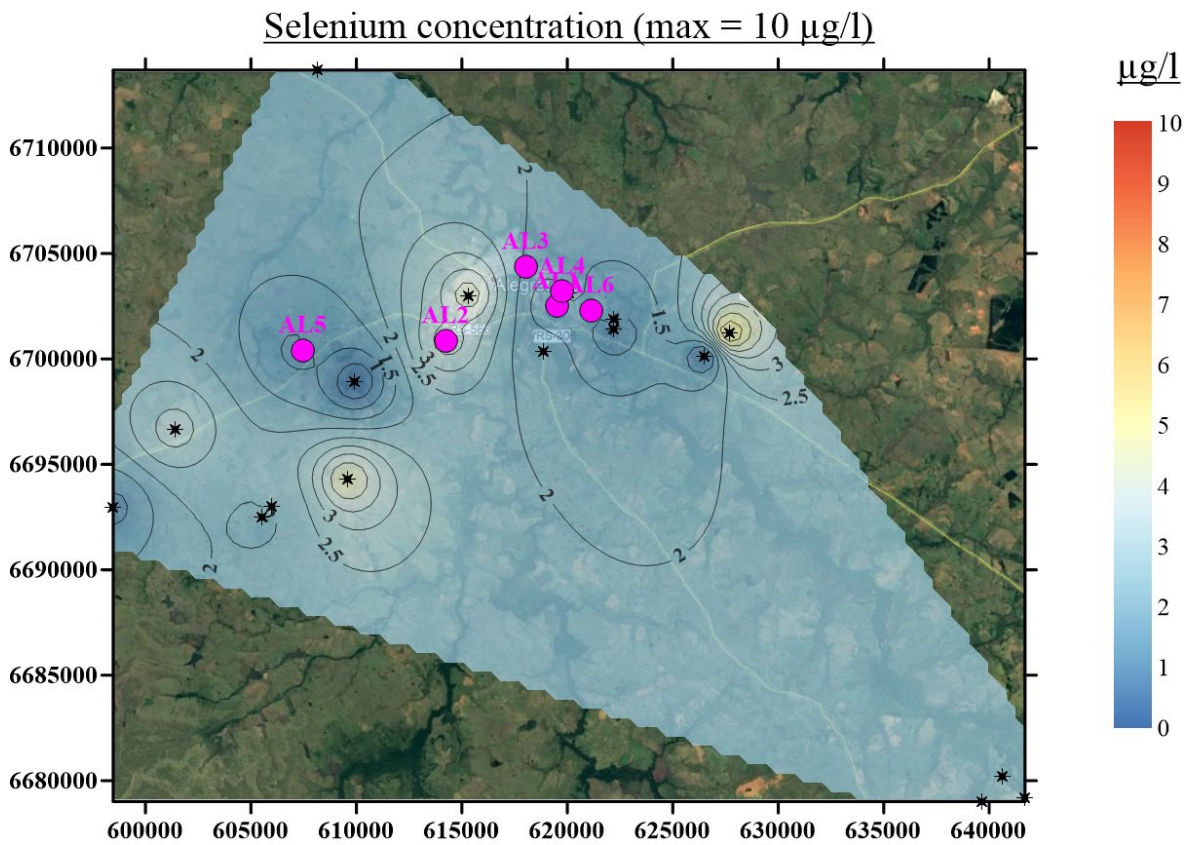
Figure 32: Selenium concentration.
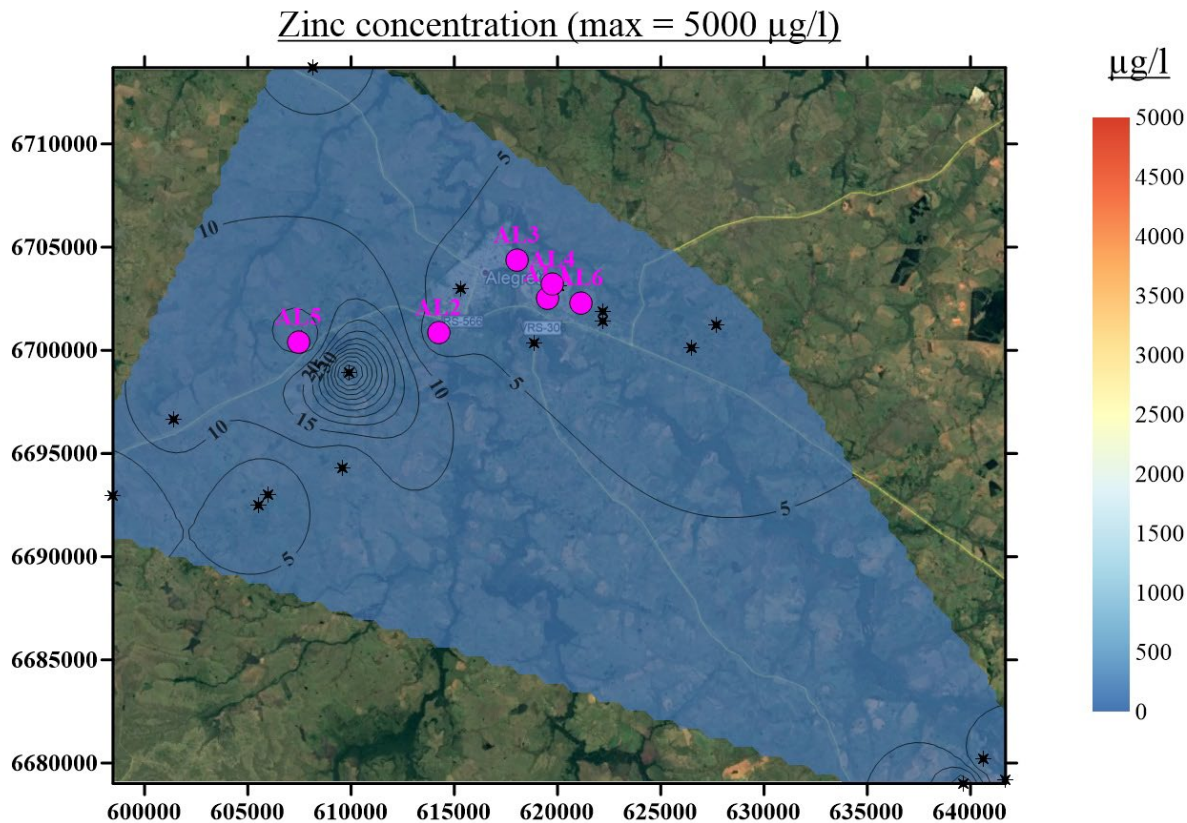
Figure 33: Zinc concentration.

mixed waters, it is believed that these waters come from geological structures of magmatic origin, probably basaltic, having rhyolite (a felsic rock) as the main contributor of calcium ions. Therefore, this result would justify the high concentration of calcium, hardness, alkalinity and magnesium in one of the regions, having the origin as a geological cause.

Geophysics

In this work it was used data from 12 surveys, divided into 6 from refraction seismic and 6 coming from electroresistivity (dipole–dipole). These two surveys were acquired concomitantly and in the same places, thus being perfectly comparable to each other. On the other hand, two of the six lines had geological information from near wells, being lines AL1 separated by 3 m from the well, whereas the second line (AL2) was 7 m apart. Additionally, the references values for Vp (Primary velocity) and Resistivity can be observed in Appendix B.

Line AL1 - Seismic Refraction and Resistivity

Figure 35 shows the inversion of the seismic data from line AL1. It indicates the presence of a very thin surface layer. In the second layer, it was found a probably basaltic lithology with a velocity above 3800 m/s that increases in depth and quickly reaches more than 7500 m/s in the third layer of the model, giving continuity to Serra Geral Formation.

The geoelectric survey of line AL1 is shown in Figure 36, showing high resistivity values corresponding to basalt in depth. Low surface resistivity may be due to wet or damp ground at the time of the data acquisition.

Line AL2 – Seismic Refraction and Resistivity

The seismic inversion of line AL2 is shown in Figure 37. Like AL1 line, a first seismic layer is presented, around few centimeters of thickness, with sandy–clayey soil, followed by weathered rocks with an approximately velocity of 1800 m/s. The third, the deepest layer, probably corresponds to a medium–grained sandstone layer as it has an approximate velocity of 3000–3400 m/s. According to the well information, this lithology is inside the Serra Geral Formation.

Piper diagram of the municipality of Alegrete
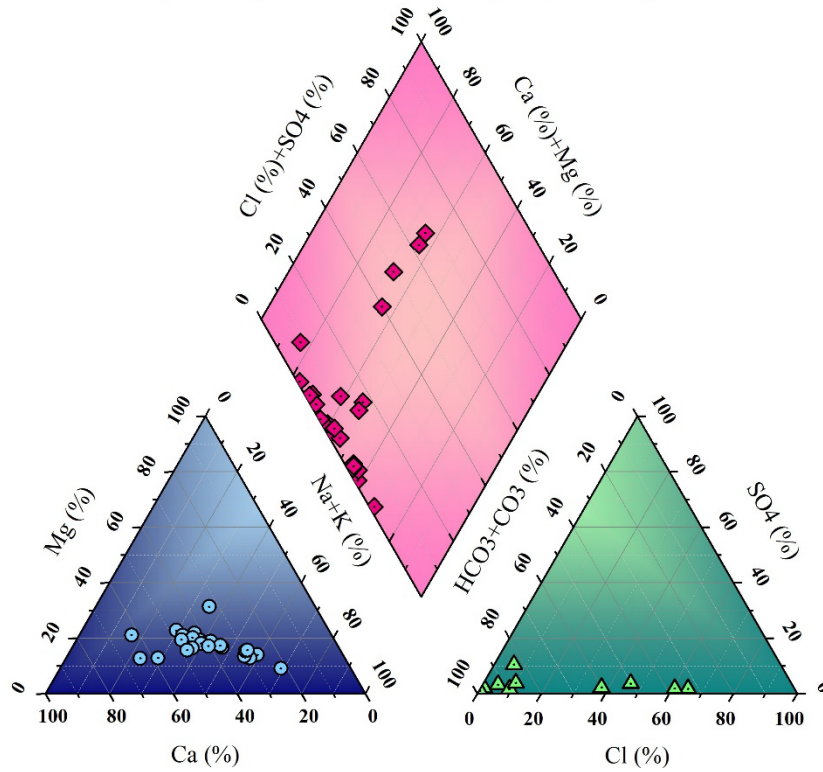
Figure 34: Piper diagram of the municipality of Alegrete.
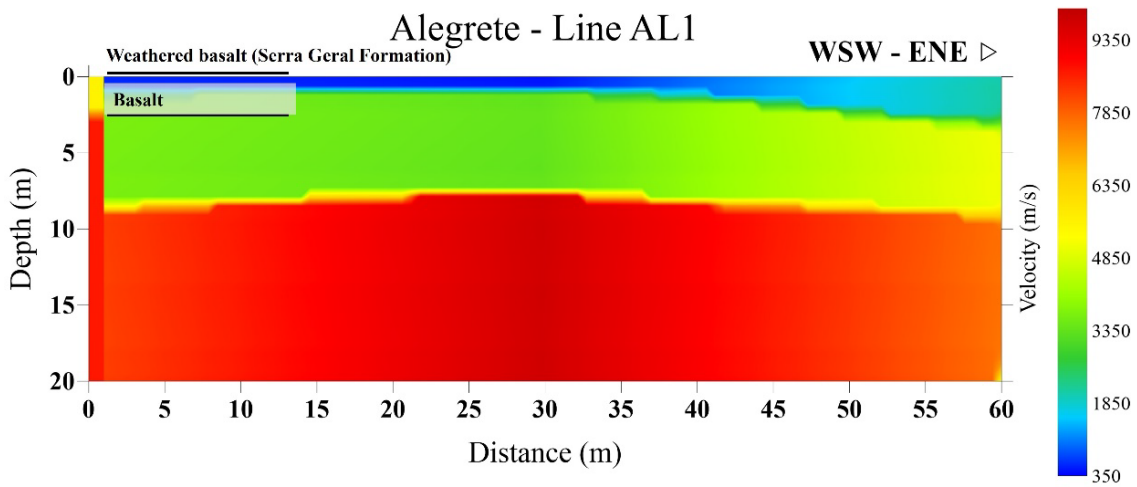
Figure 35: Line AL1 (refraction seismic inversion).
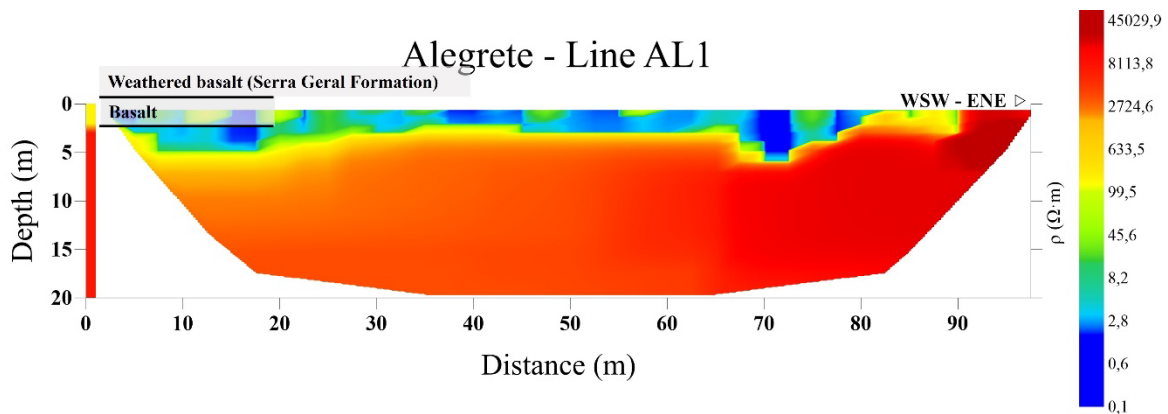
Figure 36: Line AL1 (geoelectrical survey inversion).
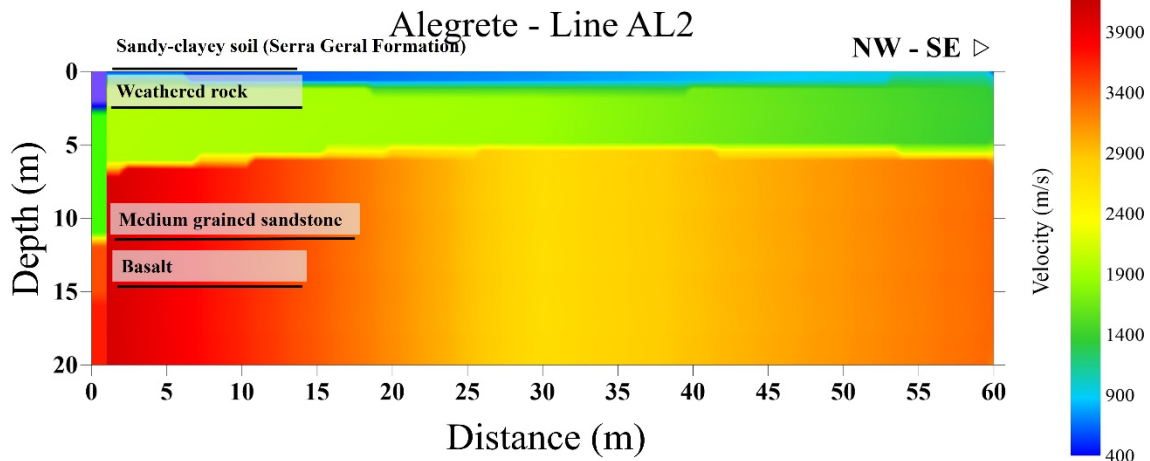
Figure 37: Line AL2 (refraction seismic inversion).

The inversion of the geoelectric survey of line AL2 is shown in Figure 38. It is noted a first layer of sandy–clayey soil with resistivity of 30 Ωm, overlapping a second layer of weathered rocks with resistivity around 90 Ωm that increases to 200 Ωm, corresponding to the average sandstone. This indicates that the basalt is at a deeper depth in this region.

Line AL3 – Seismic Refraction and Resistivity

It was observed in the seismic survey an upper layer with a velocity of 400 m/s that can be a superficial weathered rock. Next, the second layer has an approximate velocity of 3300 m/s, increasing to over 5000 m/s in the third layer. Thus, it is assumed that the second layer is the beginning of a weathered basaltic lithology, that is less altered with the increasing of depth (Figure 39).

In the geoelectric survey, it is noted a first layer that is supposed to be weathered and with a little bit of moisture, having an around 7.5 m depth and a second layer with high resistivity values being consistent with the refraction seismic survey (Figure 40).

Line AL4 – Seismic Refraction and Resistivity

Line AL4 presented high velocity values in the first meters (Figure 41). Even when the model has three layers, the weathered layer looks like having few centimeters, with a velocity over 4500 m/s at an around 6 m depth.

Observing the geoelectrical survey, it is visible the semblance between the two geophysical methods, having a first layer that seems weathered and a second at an around 6-meter depth (Figure 42), which could be basalt from Serra Geral Formation.

AL5 – Seismic Refraction and Resistivity

The inversion of the AL5 seismic survey is shown in Figure 43. It was observed a lower velocity compared to the previous lines, leading to the assumption that there was a change in lithology from basalts to sedimentary rock. The first layer was the slowest, around 300 m/s, going up to 1200 m/s in the second layer. This suggests the existence of sandy–clayey sediments, compacted in the third layer, composed of clayey sandstone.

The inversion of the resistivity survey of line AL5 is shown in Figure 44. It shows that it is a sedimentary lithology, like the interpreted in the refraction seismic survey. The average resistivity value is 190 Ωm for deeper regions, whereas on the surface the resistivity values are lower, approximately 10 Ωm.

AL6 – Seismic Refraction and Resistivity

The inversion of the AL6 seismic survey is shown in Figure 45. It presented a first layer of just a few centimeters, with a speed of 800 m/s. The second layer had a higher velocity of 2900 m/s, increasing to over 4000 m/s in the third layer. This indicates that the lithology near the surface is basalt that changes from weathered basalt to altered and completely virgin basalt at greater depths.

The inversion of the AL6 geoelectric survey is presented in Figure 46. It is shown that resistivity does not appear to be extremely high. In fact, it seems to show a depth drop of around 40–70 Ωm, at an around 10-meter depth, from SW to SE, i.e., at the right bottom of the image.
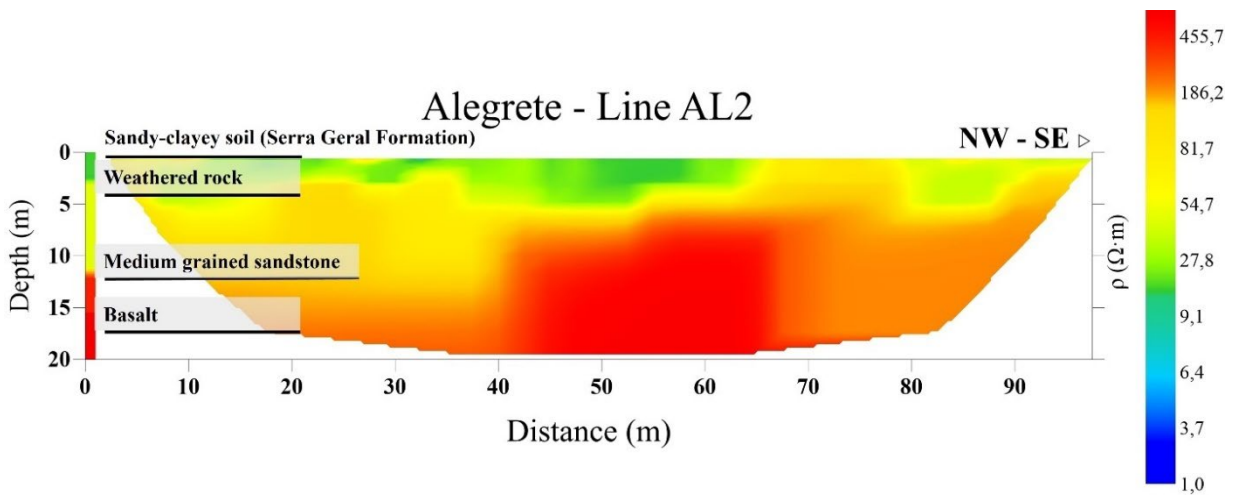
Figure 38: Line AL2 (geoelectrical survey inversion).
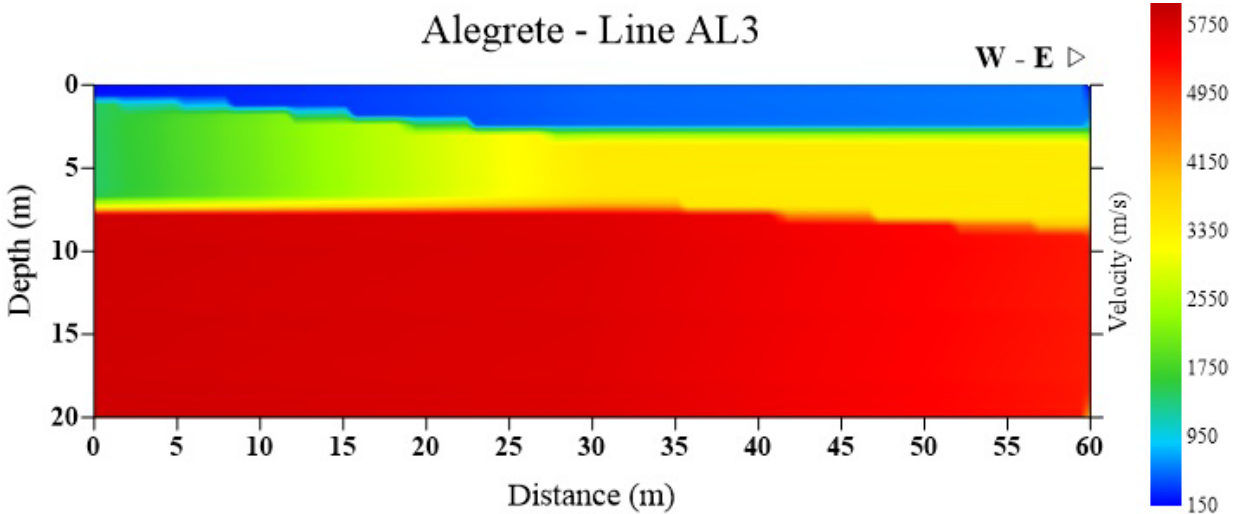
Figure 39: Line AL3 (refraction seismic inversion).
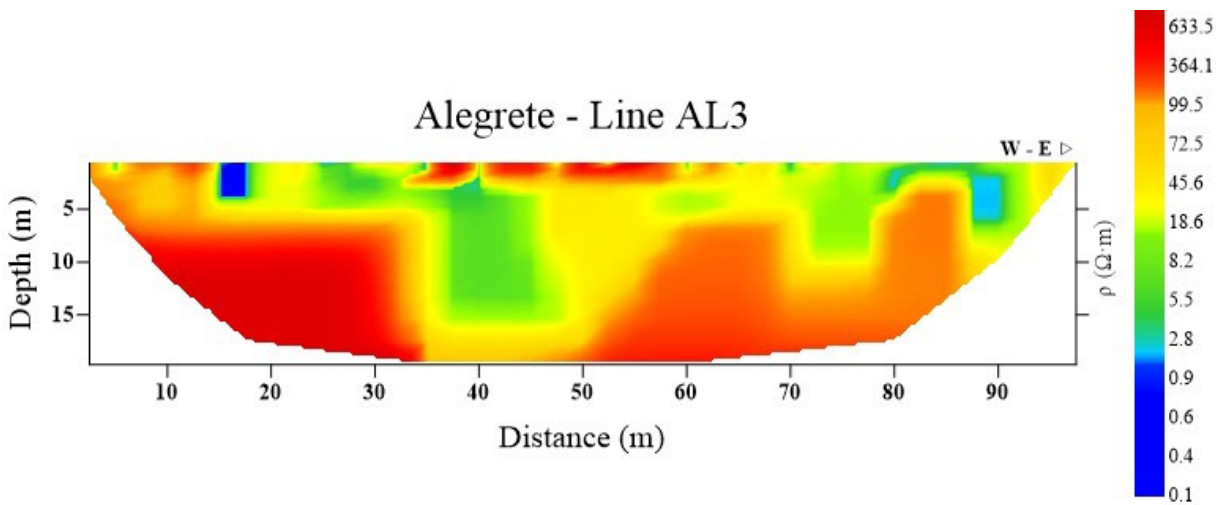
Figure 40: Line AL3 (geoelectrical survey inversion).
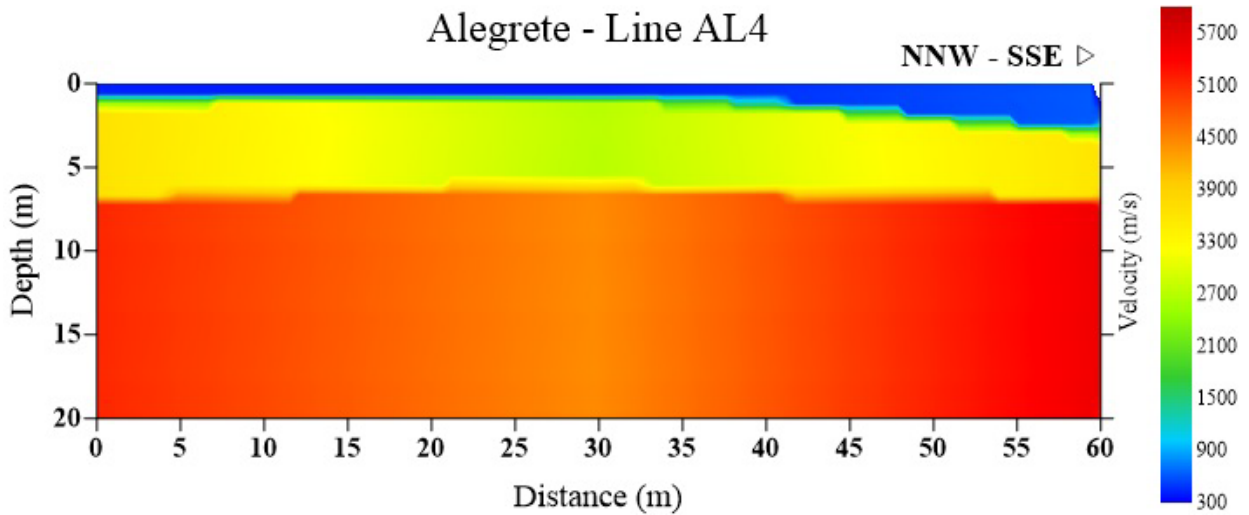
Figure 41: Line AL4 (refraction seismic inversion).
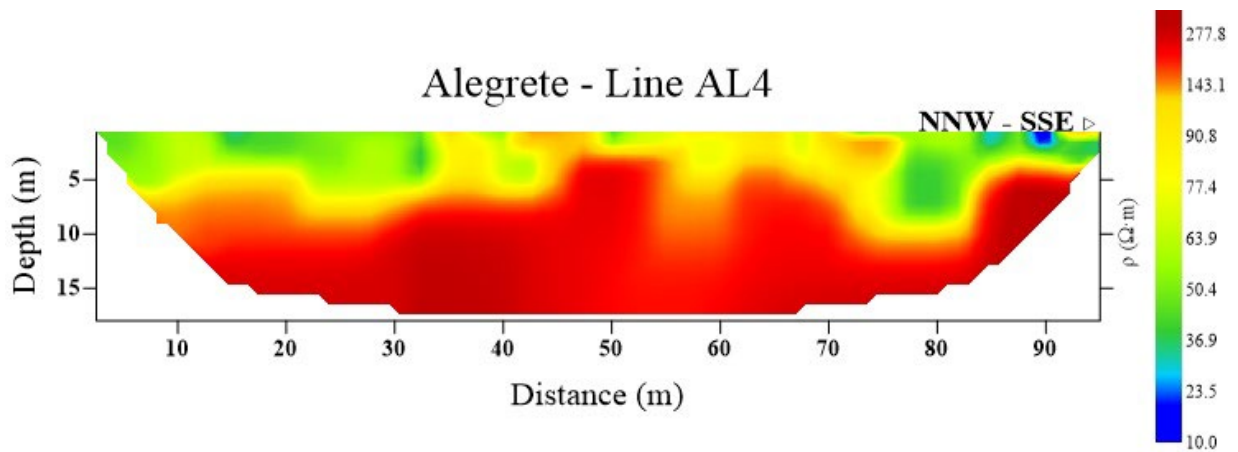
Figure 42: Line AL4 (geoelectrical survey inversion).
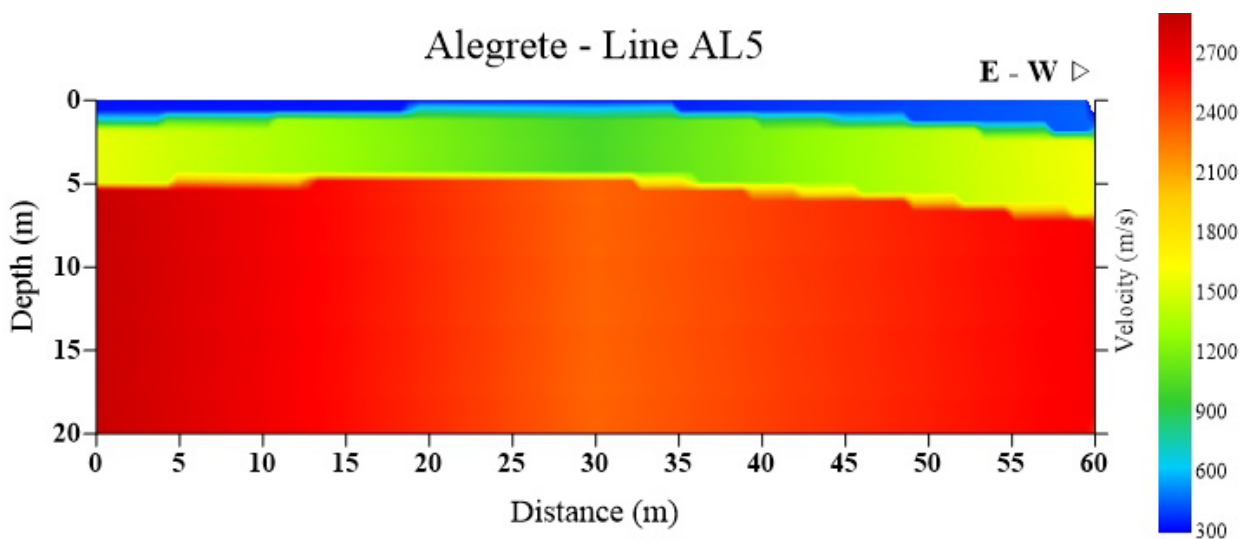
Figure 43: Line AL5 (refraction seismic inversion).
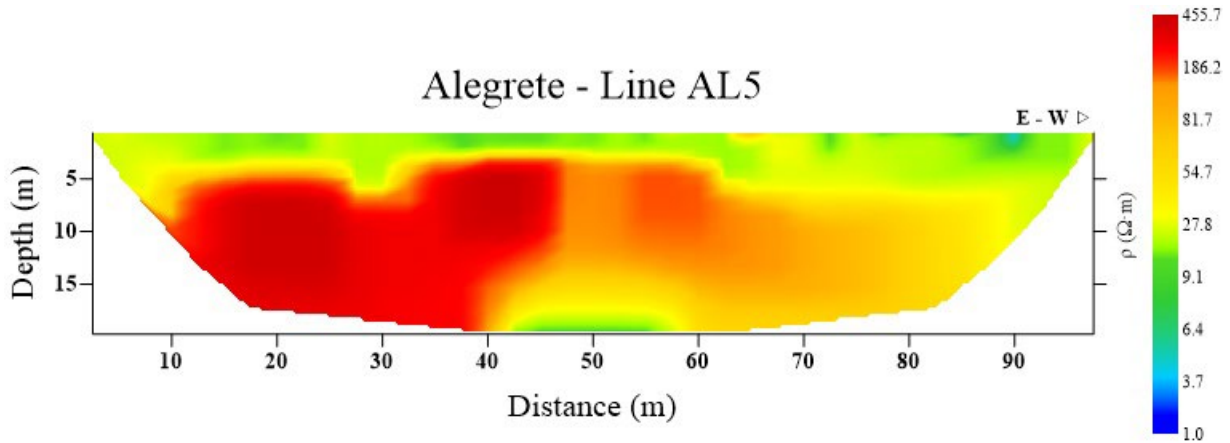
Figure 44: Line AL5 (geoelectrical survey inversion).
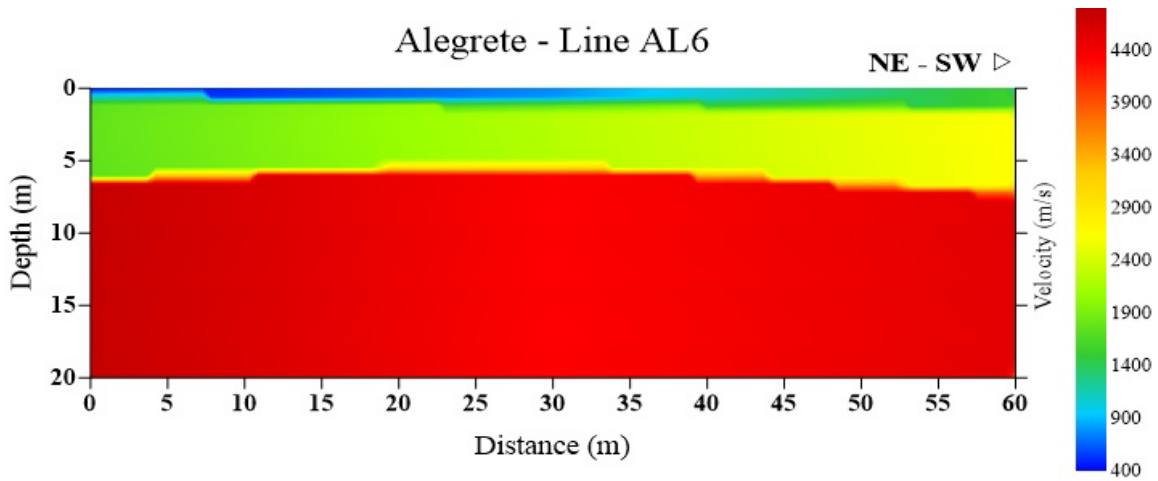
Figure 45: Line AL6 (refraction seismic inversion).
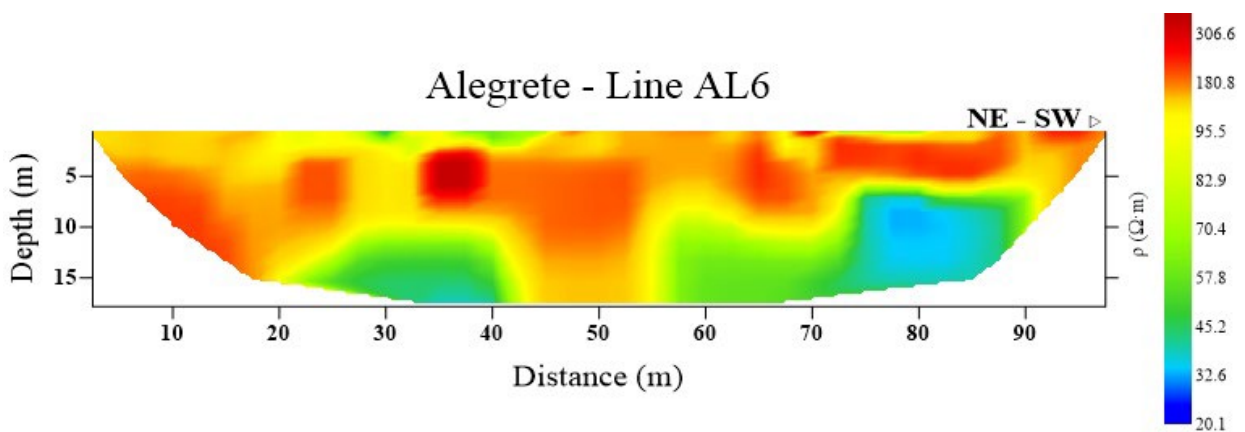
Figure 46: Line AL6 (geoelectrical survey inversion).

This may be due to the existence of fracture in the basalt, allowing water to enter and reducing the resistivity of the rock. Comparing the result of the electric survey with the seismic one, it is noted that there is coherence in the indication of the existence of basalt in the region.

Geological modelling

Geological information was taken from 92 SIAGAS wells, using the altimetry of Serra Geral and Botucatu Formations and the static level of the aquifer, delimiting the area following the same coordinates as
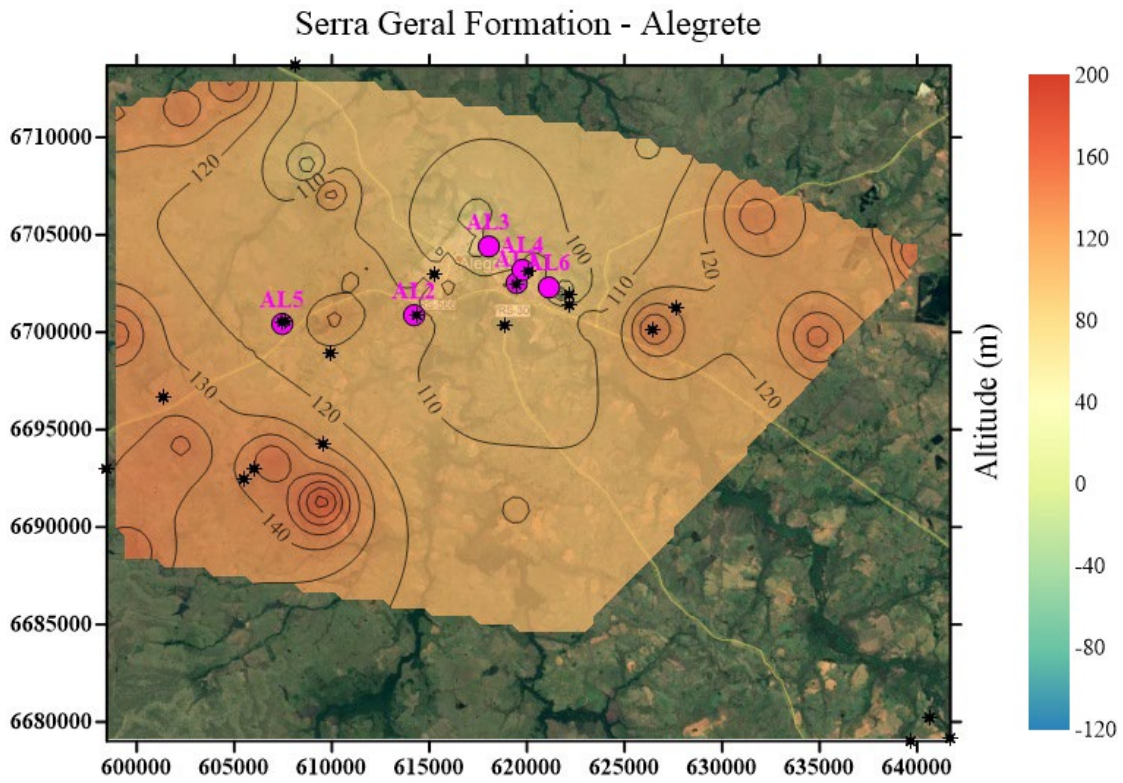
Figure 47: Contour map of Serra Geral Formation in Alegrete (pink dots indicate geophysical surveys; black stars indicate geochemical acquisition).
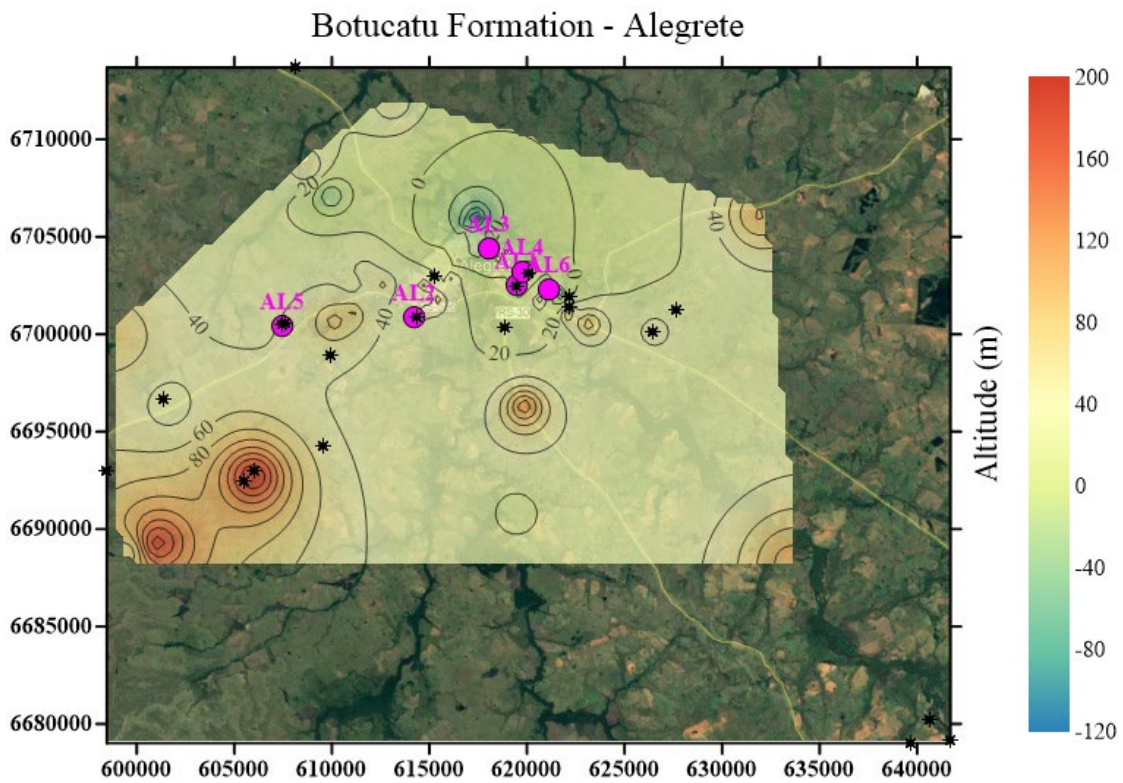
Figure 48: Contour map of Botucatu Formation in Alegrete (pink dots indicate geophysical surveys; black stars indicate geochemical acquisition).

Static level - Alegrete
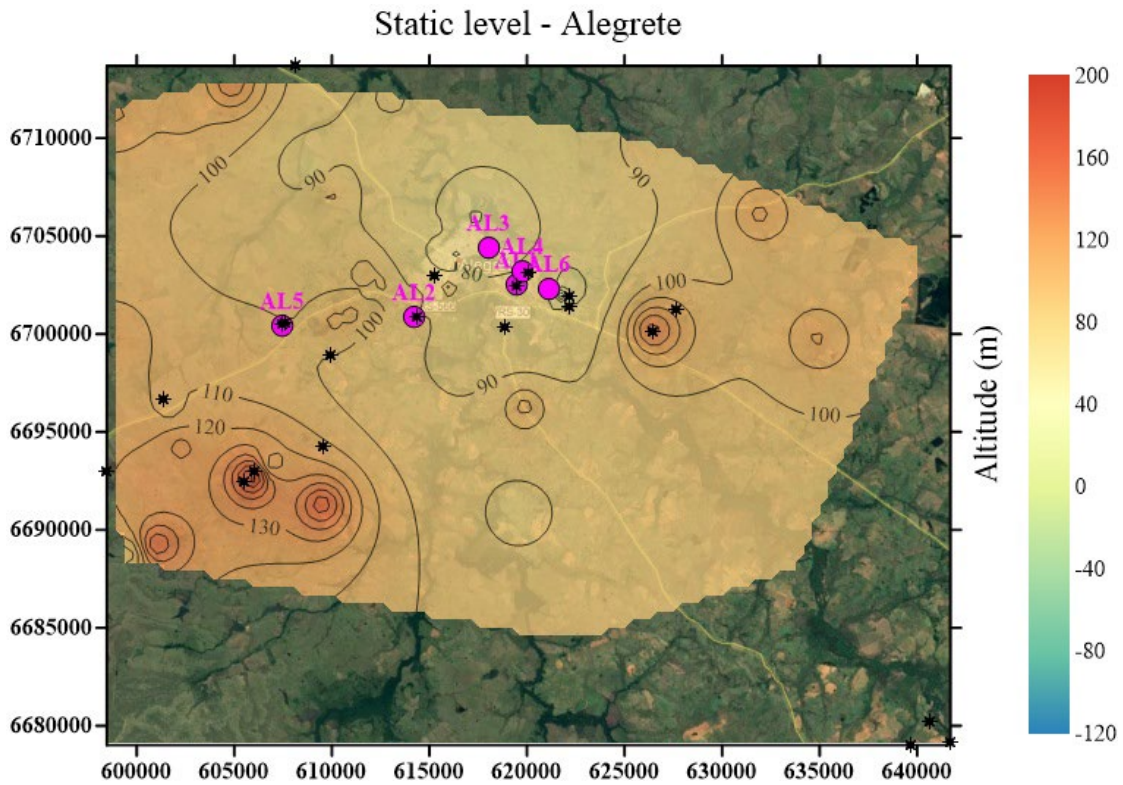
Figure 49: Contour map of the water static level of Alegrete (pink dots indicate geophysical surveys; black stars indicate geochemical acquisition).
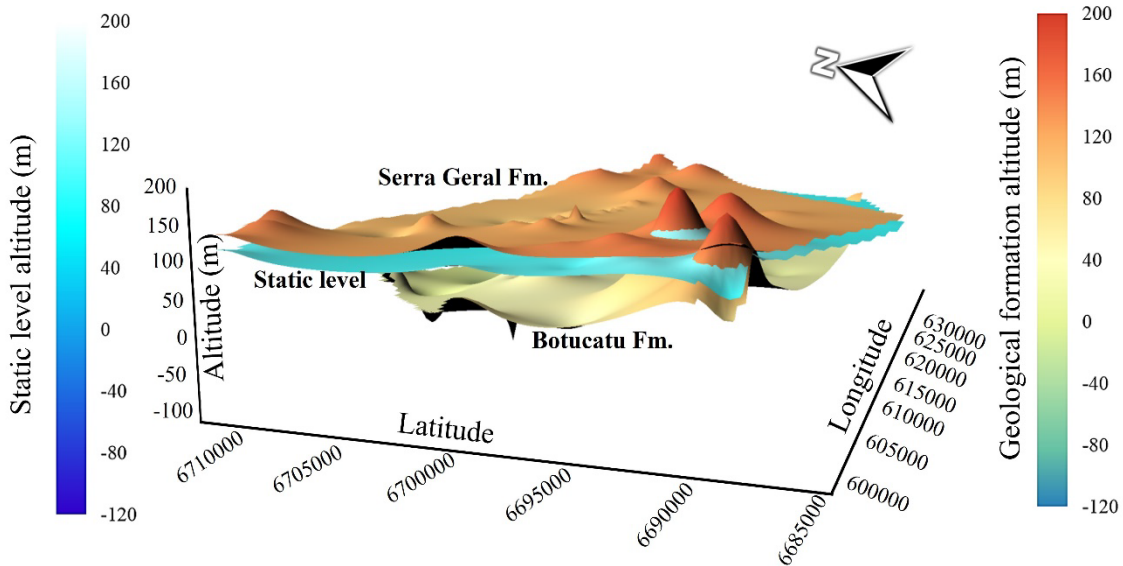
Figure 50: 3D geological modelling.

the maps of hydrogeochemical parameters to generate their respective contour maps and a 3D model

The contour maps are shown in Figures 47 and 48, respectively. In Figure 49 it is modelled the static level, that fits between the two formations. The joining of the two–dimensional models allowed the construction of a three–dimensional model of the Alegrete region, which can be seen in Figure 50. It can be clearly seen in the 3D modeling that the Serra Geral formation is located (almost always) on top of the others, suggesting that most of the aquifers in this region are probably fissural due to the basaltic geology.

CONCLUSIONS

After presenting all the results it was possible to integrate all existing data, characterizing and obtaining an overview of water quality, possible lithologies, as well as probable prospects for aquifers and how they are distributed among the different formations, functioning as a first step towards a water geo–inventory in the mentioned regions and as the basis for a water resource state plan.

The hydrogeochemical parameters in the municipality of Alegrete presented three metals that had concentrations values above their limits, which were chromium, cadmium and lead. The development of the altered hydrogeochemical parameter origin in water is as follows:

- Chromium, cadmium, lead, copper and iron: normally, these parameters are found low in normal conditions in groundwater. So, when they are excessive, their origin is anthropogenic, (possibly) from the industrial or agricultural equipment waste.

- Calcium and magnesium: they might have a geological origin, specifically in aquifers with volcanic rocks, such as basalts and rhyolites. Therefore, a high concentration of these parameters has a direct impact on water hardness, as well as on alkalinity.

The geophysics analyzes were divided into refraction seismic and geoelectric method. It was possible to get a three–layer model in refraction seismic, obtaining the first layer of weathered soil and the next two as rock layers. The geoelectric sounding coincides with the lithology and presented agreement with the results of the refraction seismic. In addition to this information, it was found the indication of a probable reservoir, as the case of AL6 line.

In addition to the above points, thanks to the well data, different formations were modeled on 2D and 3D maps, in addition to the static level of the existing aquifers.

Alternatively, it is recommended to monitor, in different seasons, the water quality and to increase the number of analyzed wells to have more certainty about the spatial variation in chemical parameters. This recommendation also applies to the geophysical surveys. Moreover, longer lines should be used to reach a larger depth.

Finally, geochemistry, geophysics and geology can be correlated. Through geophysics, it is possible to identify the layers in the subsoil and the location of reservoir prospects, which, through a chemical analysis, allow distinguishing some contaminants of water, even when biological testing has to be performed, and the probable geological origin, besides modeling the static level of the aquifer.

REFERENCES

ABNT, 2010, Amostragem de água subterrânea em poços de monitoramento — Métodos de purga [Ground water sampling in monitoring wells – Purging methods]: ABNT NBR 15847:2010, Associação Brasileira de Normas Técnicas, Brazil.

Alves, F., 2008, Estudos fitogeográficos na Bacia Hidrográfica do Arroio Lajeado Grande - Oeste do RS. Santa Maria: Master Dissertation, Universidade Federal de Santa Maria, RS, Brazil, p. 35–38, Available at: <https://repositorio.ufsm.br/bitstream/handle/1/9284/FABIANODASILVAALVES.pdf?sequence=1&isAllowed=y>, Access on: April 14, 2022.

Alves, M. G., J. L. Souza Júnior, E. L. Santos Júnior, and F. T. Almeida, 2004. Avaliação de elementos tóxicos nas águas subterrâneas no município de São Francisco de Itabapoana/RJ: Águas Subterrâneas, **1**, Available at: <https://aguassubterraneas.abas.org/asubterraneas/article/view/23355>, Access on: May 22, 2022.

ANA, 2017, Atlas Irrigação - Uso da Água na Agricultura Irrigada. Brasília, DF, Brazil. Agência Nacional de Águas, Available at: <http://arquivos.ana.gov.br/imprensa/publicacoes/AtlasIrrigacao-UsodaAguanaAgriculturaIrrigada.pdf>, Access on: April 14, 2022.

CETESB, 2022, Aquífero Guarani, Available at: <https://cetesb.sp.gov.br/aguas-subterraneas/programa-de-monitoramento/consulta-por-aquiferos-monitorados/aquifero-guarani>, Access on: May 22, 2022

Clesceri, L., A. Greenberg, and A. Eaton, 1998, Standard Methods for the Examination of Water and Wastewater: American Public Health Association – APHA, 20th ed., UCLA, United States.

CONAMA, 2008, Resolução CONAMA no 396, de 3 de abril de 2008. Dispõe sobre a classificação e diretrizes ambientais para o enquadramento das águas subterrâneas e dá outras providências. Conselho Nacional do Meio Ambiente. Ministério do Meio Ambiente. Brasília, DF, Brazil, Available at: <http://conama.mma.gov.br/?option=com_sisconama&task=arquivo.download&id=545>, Access on: April 14, 2022.

CPRM, 2008, Projeto de Proteção Ambiental e Desenvolvimento Sustentável do Sistema Aqüifero Guarani – PSAG, Available at: <http://www.cprm.gov.br/publique/Noticias/Projeto-de-Protecao-Ambiental-e-Desenvolvimento-Sustentavel-do-Sistema-Aquifero-Guarani---PSAG-938.html>, Access on: May 22, 2022.

De Paula, PM., 2006, Mapeamento de Unidades Litomorfológicas em Bacias Hidrográficas com Processos de Arenização, Alegrete – RS: MSc. Dissertation. UFRGS, RS, Brazil. 2006. 69 pp.

De Paula, P. M., and L. E. Robaina, 2003, Mapeamento de Unidades Geológicas-Geomorfológicas da Bacia do Arroio Lajeado Grande – RS: Geociências, **22**, 2, pp. 3–9.

Dondurur, D., 2018, Velocity Analysis: Acquisition and Processing of Marine Seismic Data: Elsevier. Chapter 9, 421–457, Access on: May 22, 2022, Available at: 10.1016/B978-0-12-811490-2.00009-8.

ENRESS, 2018, Ley 11.220 - Anexo A - Limites para la Provision de Agua Potable: El Ente Regulador de Servicios Sanitarios, Santa Fe, Argentina, Available at: <http://www.enress.gov.ar/wp-content/uploads/2018/01/LEY-11.220-ANEXO-A.pdf>, Access on: April 14, 2022.

FAO, 2005, Decreto Nº 32.327/S - Reglamento para la Calidad del Agua Potable: La Gaceta Número 84, May 3, 2005, Food and Agriculture Organization, Costa Rica, Available at: <http://extwprlegs1.fao.org/docs/pdf/cos73577.pdf>, Access on: April 14, 2022.

Flores Machado, J. L., 2005, Compartimentação Espacial e Arcabouço Hidroestratigráfico do Sistema Aquífero Guarani no Rio Grande do Sul: PhD Thesis. UNISINOS, RS, Brazil.

García, J., N. López, and J. Muñoz, 2011, Aplicación de la Prospección Geofísica Utilizando el Método Schlumberger para la Exploración del Agua Subterránea en Canton los Magueyes, Colonia Santa Lucia, Municipio de Ahuachapán: Undergraduate Final Project, Universidad de El Salvador, Available at: <http://ri.ues.edu.sv/id/eprint/458/1/10136842.pdf>, Access on: April 14, 2022.

Gleick, P. H., L. Nicholas, D. H. Cain, C. Henges-Jeck, C. Hunt, M. Kiparsky, M. Moench, and G. H. Wolff, 2004, The World's Water, 2004-2005: The Biennial Report on Freshwater Resources, Washington D.C., Island Press, 262 pp.

Glover, P. W. J., 2015, Geophysical Properties of the Near Surface Earth: Electrical Properties: Treatise on Geophysics, 2nd ed., **11**, 89–137, doi: 10.1016/B978-0-444-53802-4.00189-5

Health Canada, 2019, Cadmium in Drinking Water: Guideline Technical Document for Public Consultation, Ottawa, Canada, Available at: <https://www.canada.ca/content/dam/hc-sc/images/programs/consultation-cadmium-drinking-water/Cadmium_in_Drinking_Water_01-29-2019_ENG.pdf>, Access on: April 14, 2022.

IBGE, 2020a, Cidades@, Rio Grande do Sul – Alegrete: Produção Agrícola - Lavoura Temporária: Arroz: Instituto Brasileiro de Geografia e Estatística, Brazil, Available at: <https://cidades.ibge.gov.br/brasil/rs/alegrete/pesquisa/14/10193?tipo=ranking&indicador=10368>, Access on: January 24, 2022.

IBGE, 2020b, Cidades@, Rio Grande do Sul – Alegrete: Pecuária: Instituto Brasileiro de Geografia e Estatística, Brazil, Available at: <https://cidades.ibge.gov.br/brasil/rs/alegrete/pesquisa/18/0?tipo=ranking&indicador=16541>, Access on: January 24, 2022.

Martins, L. C., W. Wildner, and L. A. Hartimann, 2011, Estratigrafia dos derrames da Província Vulcânica Paraná na região oeste do Rio Grande do Sul, Brasil, com base em sondagem, perfilagem gamaespectrométrica e geologia de campo: Pesquisas em Geociências, **38**, 1, 15–27, doi: 10.22456/1807-9806.23833.

MPCA, 1999, Copper, Chromium, Nickel and Zinc in Minnesota's Ground Water: Minnesota Pollution Control Agency, Available at: <https://www.pca.state.mn.us/sites/default/files/copper7.pdf>, Access on: April 14, 2022.

Orellana, E., 1982, Prospección Geoeléctrica en corriente continua: Madrid, Paraninfo, Biblioteca Técnica Philips, 523 pp.

Pinheiro, A., V. Kaufmann, D. Schneiders, D. A. de Oliveira, and R. M. Albano, 2013, Concentrações e cargas de nitrato e fosfato na Bacia do Ribeirão Concórdia, Lontras, SC: Revista Brasileira de Engenharia Agrícola e Ambiental, **17**, 1, 86–93, doi: 10.1590/S1415-43662013000100012.

Portal de Tratamento de Água, 2008, Parâmetros Analíticos, Available at: <https://www.tratamentodeagua.com.br/artigo/parametros-analiticos>, Access on: April 14, 2022.

Raju, P., M. Reddy, P. Raghuram, G. Babu, T. Rambabu, and J. Jeevan Kumar, 2014, Alkalinity and Hardness Variation in Ground Waters of East Godavari District due to Aquaculture: International Journal of Fisheries and Aquatic Studies, IJFAS, **1**, 6, 121–127.

Rao, N. S., and P. R. Prasad, 1997, Phosphate pollution in the groundwater of lower Vamsadhara river basin, India: Environmental Geology, **31**, 117–122, doi: 10.1007/s002540050170.

Soares, G. B., 2019, Caracterização hidroquímica de águas subterrâneas aliada ao uso de óxido de grafeno reduzido para adsorção de herbicidas: PhD Thesis, PUCRS, RS, Brazil, 150 pp.

SPGG, 2019, Atlas Socioeconômico do Rio Grande do Sul, RS, Brazil: Secretaria de Planejamento, Governança e Gestão – SPGG, Available at:

<https://atlassocioeconomico.rs.gov.br/vab-da-agropecuaria>, Access on: December 20, 2018.

Telford, W., L. Geldart, and R. Sheriff, 1990, Applied Geophysics: 2nd ed., Cambridge University Press, 792 pp, doi: 10.1017/CBO9781139167932.

Tiecher T., Org., 2017, Manejo e conservação do solo e da água em pequenas propriedades rurais no sul do Brasil: impacto das atividades agropecuárias na contaminação do solo e da água: Universidade Regional Integrada do Alto Uruguai e das Missões, Editora URI, Frederico Westphalen, RS, Brazil, 181 pp. Available at: <https://www.researchgate.net/publication/334041443_Manejo_e_conservacao_do_solo_e_da_agua_em_pequenas_propriedades_rurais_no_sul_do_Brasil_impacto_das_atividades_agropecuarias_na_contaminacao_do_solo_e_da_agua>, Access on: May 22, 2022.

UNESCO, 2018, The United Nations world water development report 2018: nature-based solutions for water: United Nations Educational, Scientific and Cultural Organization, UNESCO World Water Assessment Programme, Available at: <https://unesdoc.unesco.org/ark:/48223/pf0000261424>, Access on: May 22, 2022.

Welch, H., J. Kingsbury, and R. Coupe, 2010, Effects of the biofuels initiative on water quality and quantity in the Mississippi Alluvial Plain: Mississippi Water Resources Conference, St. Louis, Mississippi, United States, p. 142–155

Wick, K., C. Heumesser, and E. Schmid, 2012, Groundwater nitrate contamination: factors and indicators: Journal of Environmental Management, **111**, 3, 178–186, doi: 10.1016/j.jenvman.2012.06.030.

Zalán, P., S. Wolff, J. Conceição, M. Astolfi, I. Vieira, V. Appi, and O. Zanotto, 1987, Tectônica e sedimentação da Bacia do Paraná: Simpósio Sul-Brasileiro de Geologia, 1, Curitiba, PR, Brazil, Available at: <https://www.researchgate.net/publication/288353057_Tectonica_e_sedimentacao_da_Bacia_do_Parana>, Access on: April 14, 2022.

APPENDIX A – MAXIMUM HYDROGEOCHEMICAL VALUES

Parameter	Maximum value mgl=1ppm=1000µgl	Reference
Alkalinity	200	(ENRESS, 2018)
Aluminum (Al)	0.2	(CONAMA, 2008)
Arsenic (As)	0.01	(CONAMA, 2008)
Barium (Ba)	0.7	(CONAMA, 2008)
Cadmium (Cd)	0.001	(Health Canada, 2019)
Calcium (Ca+)	100	(ENRESS, 2018)
Lead (Pb)	0.1	(CONAMA, 2008)
Chloride (Cl-)	250	(CONAMA, 2008)
Copper (Cu)	2	(CONAMA, 2008)
Chromium (Cr)	0.5	(CONAMA, 2008)
Water Hardness	500	(CONAMA, 2008)
Iron (Fe)	0.3	(CONAMA, 2008)
Fluoride (F-)	1.5	(CONAMA, 2008)
Phosphate (PO4-3)	0.45	(Pinheiro et al., 2013)
Magnesium (Mg2+)	30	(ENRESS, 2018)
Manganese (Mn)	0.1	(CONAMA, 2008)
Nitrate (NO3-)	10	(CONAMA, 2008)
Dissolved oxygen	6	(CONAMA, 2008)
Potassium (K+)	10	(FAO, 2005)
Selenium (Se)	0.01	(CONAMA, 2008)
Sodium (Na+)	200	(CONAMA, 2008)
Sulfate (SO4-)	250	(CONAMA, 2008)
Zinc (Zn)	5	(CONAMA, 2008)

APPENDIX B - REFERENCE VALUES OF VP AND RESISTIVITY (Glover, 2015; Dondurur, 2018)

Material	Vp (m/s)	Resistivity (Ωm)
Water	1450–1530	10–100
Alluvial sediments	1800–2200	10–800
Saturated sand	1500–2000	30–150
Dry sand	400–1200	80–1050
Sandstone	1400–4500	$1 – 7.4 \times 10^8$
Clay	1000–2500	1–2000
Clayey sand	–	30–215
Clayey soil	–	8–33
Basalt	5500–6500	$10–1.3 \times 10^7$
Limestone	3000–6000	50–107
Dolomite	2500–6500	$350–5 \times 10^3$
Granite	4500–6000	$5000–1.3 \times 10^6$
Unconsolidated sediments	100–500	8–1700
Schist	2000–4100	$10–10^4$